 Related Commentary, page 4618

T cell protein tyrosine phosphatase attenuates T cell signaling to maintain tolerance in mice

Florian Wiede,[1] Benjamin J. Shields,[1] Sock Hui Chew,[1] Konstantinos Kyparissoudis,[2] Catherine van Vliet,[1] Sandra Galic,[1] Michel L. Tremblay,[3] Sarah M. Russell,[4,5] Dale I. Godfrey,[2] and Tony Tiganis[1]

[1]Department of Biochemistry and Molecular Biology, Monash University, Clayton, Victoria, Australia. [2]Department of Microbiology and Immunology, University of Melbourne, Parkville, Victoria, Australia. [3]McGill Cancer Centre and Department of Biochemistry, McGill University, Montreal, Quebec, Canada. [4]Immune Signaling Laboratory, Cancer Immunology, Peter MacCallum Cancer Centre, East Melbourne, Victoria, Australia. [5]Centre for MicroPhotonics, Swinburne University of Technology, Hawthorn, Victoria, Australia.

Many autoimmune diseases exhibit familial aggregation, indicating that they have genetic determinants. Single nucleotide polymorphisms in *PTPN2*, which encodes T cell protein tyrosine phosphatase (TCPTP), have been linked with the development of several autoimmune diseases, including type 1 diabetes and Crohn's disease. In this study, we have identified TCPTP as a key negative regulator of TCR signaling, which might explain the association of *PTPN2* SNPs with autoimmune disease. We found that TCPTP dephosphorylates and inactivates Src family kinases to regulate T cell responses. Using T cell–specific TCPTP-deficient mice, we established that TCPTP attenuates T cell activation and proliferation in vitro and blunts antigen-induced responses in vivo. TCPTP deficiency lowered the in vivo threshold for TCR-dependent $CD8^+$ T cell proliferation. Consistent with this, T cell–specific TCPTP-deficient mice developed widespread inflammation and autoimmunity that was transferable to wild-type recipient mice by $CD8^+$ T cells alone. This autoimmunity was associated with increased serum levels of proinflammatory cytokines and anti-nuclear antibodies, T cell infiltrates in non-lymphoid tissues, and liver disease. These data indicate that TCPTP is a critical negative regulator of TCR signaling that sets the threshold for TCR-induced naive T cell responses to prevent autoimmune and inflammatory disorders arising.

Introduction

The development of T cells in the thymus, the maintenance of a peripheral T cell repertoire, and the activation of T cells in secondary lymphoid organs rely on T cells recognizing antigen via the TCR. The MHC-restricted TCR complex comprises TCRα, -β, and -ζ subunits and three invariant CD3 polypeptides (γ, δ, ε) and can operate in conjunction with the CD4 or CD8 coreceptors (1). When the TCR engages its cognate peptide-MHC (pMHC) on antigen-presenting cells, the Src family protein tyrosine kinases (SFKs) Lck and Fyn are activated (1–3). CD4 and CD8 serve to enhance the recruitment of Lck to the TCR, but high-affinity ligands can signal independently of these coreceptors (3–5). Active SFKs phosphorylate TCRζ and CD3ε, allowing for the recruitment of the tyrosine kinase ZAP-70 (ζ chain–associated protein kinase of 70 kDa), which in turn is phosphorylated and activated by Lck to instigate effector cascades that promote gene expression, proliferation, and differentiation (1–3). The principal role of Lck in TCR signaling is highlighted by the severely disrupted thymocyte development and vastly reduced peripheral T cell numbers in Lck-deficient mice (6). Moreover, Lck is essential for naive T cell clonal expansion and the acquisition of effector functions in the periphery (2, 3, 7–9).

The duration and strength of the TCR signal propagated by Lck and ZAP-70 control T cell development in the thymus (2, 3). Thymocytes are selected based on their affinity for self-pMHC and the resulting intensity of TCR signaling (4, 10, 11); thymocytes with high-affinity TCRs that are capable of developing into autoreactive T cells undergo programmed cell death in a process known as negative selection, whereas those with low to moderate affinity develop further in a process known as positive selection (10). In the periphery, TCR recognition of foreign peptide antigen presented by MHC and the activation of Lck are essential in the initiation of naive T cell responses to invading pathogens, inducing clonal expansion, cytokine production, and the acquisition of effector functions (2, 3, 7–9). The affinity of the TCR for the presented foreign pMHC, the kinetics of the TCR-pMHC interaction, and the number of receptors engaged determine the strength of the TCR signal and the robustness of the T cell response (12–16). Productive T cell responses to foreign antigen are dependent on co-stimulation, the most common being that mediated by CD28 when it engages CD80/CD86 on activated antigen-presenting cells (1). Co-stimulation serves to quantitatively increase TCR/SFK signaling, allowing for the production of IL-2 and expression of the IL-2 receptor to promote T cell survival and to drive clonal expansion and effector development (1, 17).

Protein tyrosine phosphatases (PTPs) are important in T cell development and function and contribute to both the promotion and attenuation of T cell signaling. For example, the receptor type PTP CD45 is required for Lck activation and the promotion of TCR signaling (18–20). CD45 also regulates basal and TCR-instigated Lck Y394 autophosphorylation (21–23) and inhibits TCR signaling. Other PTPs have also been implicated in Lck Y394 dephosphorylation. Several lines of evidence point to SHP-1 being important in Lck inactivation, but conflicting studies suggest that SHP-1 does not suppress TCR-induced Lck activation and instead dephosphorylates LAT or ZAP-70 (24–27). LYP/PEP (encoded by *PTPN22*) has been shown to act directly on Lck Y394 in a cellular context (28), and TCR-induced Lck Y394 and ZAP-70 phosphorylation and downstream signaling and proliferation are elevated in effector/memory T cells from *Ptpn22*$^{-/-}$ mice (29). The importance of PTPs in regulating TCR signaling is underscored by the poten-

Conflict of interest: The authors have declared that no conflict of interest exists.
Citation for this article: *J Clin Invest.* 2011;121(12):4758–4774. doi:10.1172/JCI59492.

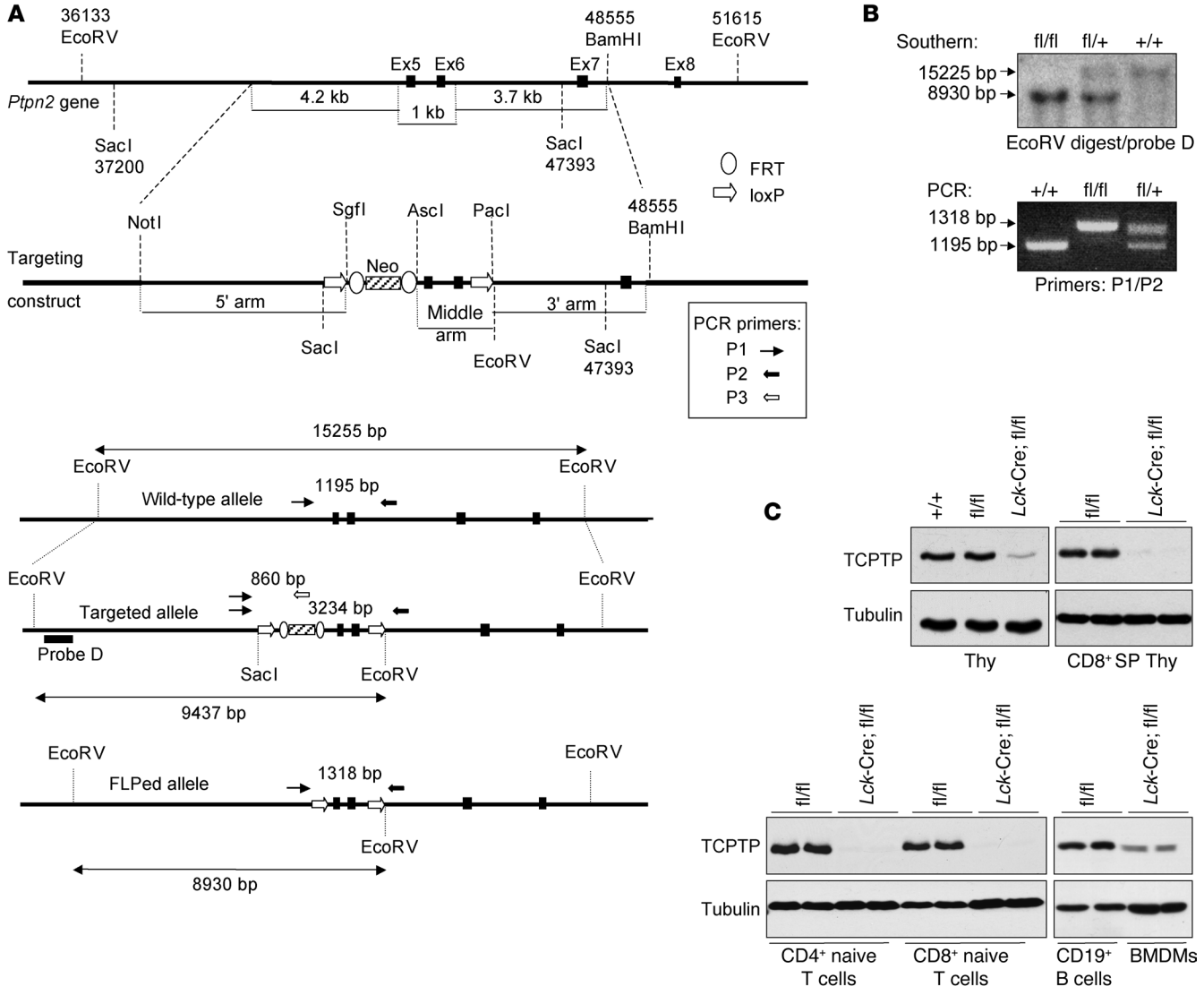

Figure 1

Generation of *Lck*-Cre;*Ptpn2*$^{fl/fl}$ mice. (**A**) *Ptpn2* genomic locus and targeting design. (**B**) Southern blot and PCR analysis of wild-type and *Ptpn2* floxed mice. (**C**) TCPTP expression in *Ptpn2*$^{fl/fl}$ (fl/fl) and *Lck*-Cre;*Ptpn2*$^{fl/fl}$ (*Lck*-Cre; fl/fl) thymocytes (Thy), FACS-purified CD8$^+$SP thymocytes, and CD4$^+$ or CD8$^+$ LN naive T cells and MACS purified CD19$^+$ splenic B cells, as well as bone marrow–derived macrophages (BMDMs). Results are representative of at least 3 independent experiments.

tial for human disease when PTP function is perturbed. For example, CD45 deficiency leads to severe combined immunodeficiency (30, 31), whereas a SNP in *PTPN22* contributes to the development of autoimmune diseases, including type 1 diabetes, rheumatoid arthritis, systemic lupus erythematosus, and Graves disease (32).

PTPN2, encoding T cell PTP (TCPTP), has been identified as a susceptibility locus for autoimmune diseases. SNPs in *PTPN2* have been linked to the development of type 1 diabetes, rheumatoid arthritis, and Crohn's disease (33–35). Recently, the type 1 diabetes–linked *PTPN2* variant rs1893217(C) has been associated with decreased *PTPN2* expression in T cells (36). Deletion of the *PTPN2* gene has also recently been implicated in the development of T cell acute lymphoblastic leukemias (37). Previous studies have shown that *Ptpn2*$^{-/-}$ mice develop symptoms of progressive systemic inflammatory disease by 1–2 weeks of age and die from severe anemia attributed to a defective bone microenvironment at 3–5 weeks of age (38, 39). However, the morbidity and mortality associated with global TCPTP deficiency preclude detailed analyses of T cell responses in *Ptpn2*$^{-/-}$ mice. Here we have conditionally deleted *Ptpn2* in T cells and demonstrate that TCPTP attenuates TCR signaling and sets the threshold for T cell activation. Our studies provide insight into a key mechanism for T cell tuning for the prevention of immune and inflammatory disorders.

Results

Generation of Lck-Cre;Ptpn2$^{fl/fl}$ *mice*. We generated a floxed allele of *Ptpn2* (*lox*P sites flanking exons 5 and 6 encoding the core of the catalytic domain including the catalytically essential Asp182 and Cys216 residues; Figure 1, A and B) by gene targeting in Bruce-4 embryonic stem cells and conditionally ablated TCPTP using the

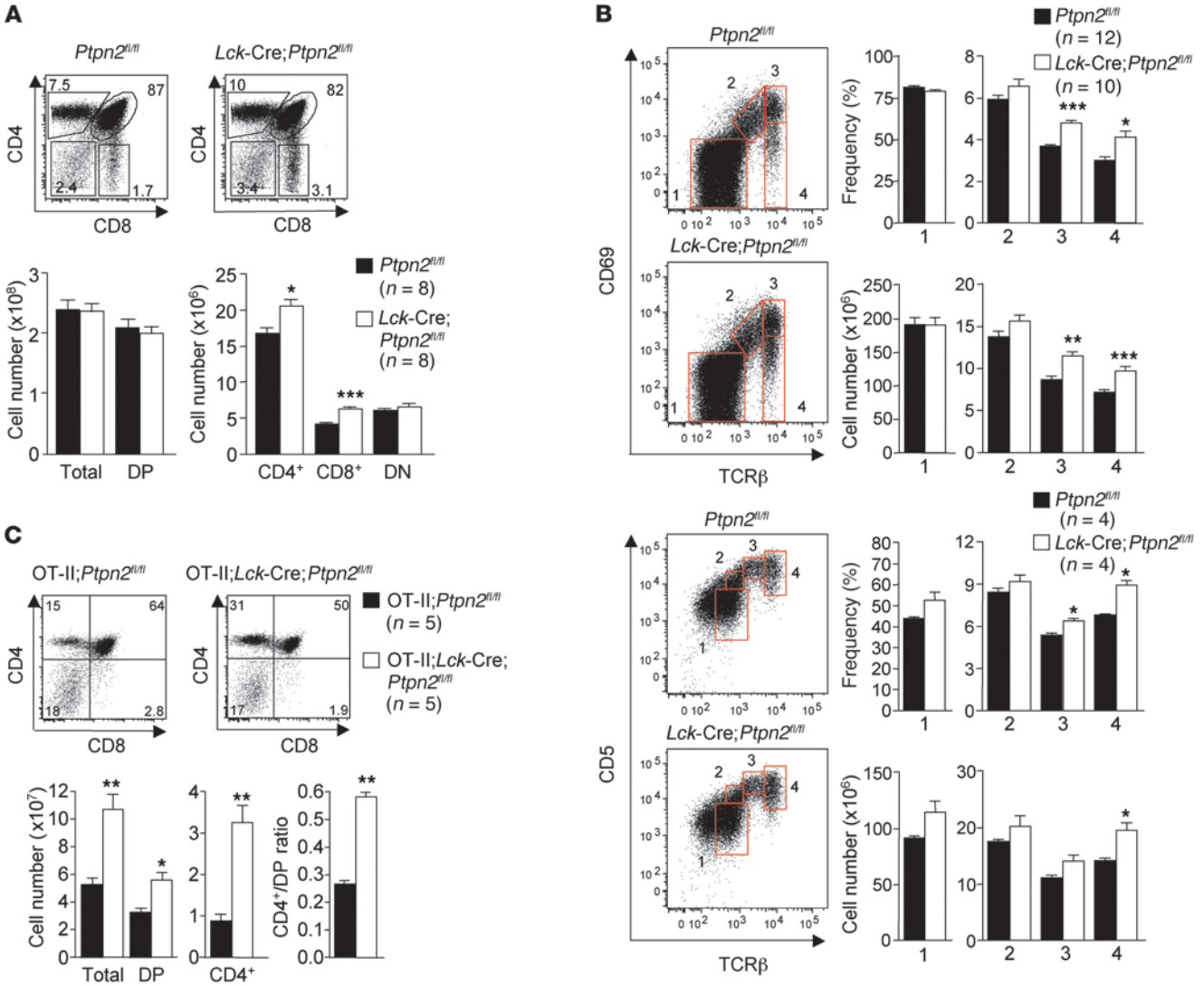

Figure 2

Thymocyte development in *Lck*-Cre;*Ptpn2*$^{fl/fl}$ mice. *Ptpn2*$^{fl/fl}$ and *Lck*-Cre;*Ptpn2*$^{fl/fl}$ thymocytes from 4-week-old mice were stained with fluorochrome-conjugated α-CD4, -CD8, -TCRβ, -CD69, and -CD5 and analyzed by flow cytometry. (**A**) Representative dot blots (numbers in outlined areas are percentages of cells in gate) and results from 3 experiments are shown. (**B**) Cells were gated for the different developmental stages (labeled 1–4) according to the expression of the positive selection markers CD69, CD5, and TCRβ, and absolute numbers were determined. Representative dot blots and results from 3 experiments are shown. (**C**) Thymocytes from OT-II TCR transgenic *Ptpn2*$^{fl/fl}$ (OT-II;*Ptpn2*$^{fl/fl}$) and *Lck*-Cre;*Ptpn2*$^{fl/fl}$ (OT-II;*Lck*-Cre;*Ptpn2*$^{fl/fl}$) mice were stained with fluorochrome-conjugated α-CD4 and α-CD8 and analyzed by flow cytometry. Cells were gated for the DP and CD4$^+$SP stages, and absolute numbers and the indicated ratios were determined. Representative dot plots (numbers in outlined areas are percentages of cells in gate) and results from 2 independent experiments are shown. Results in **A**–**C** are mean ± SEM for the indicated numbers of mice; significance was determined using a 2-tailed Mann-Whitney *U* test; $^*P < 0.05$, $^{**}P < 0.01$, $^{***}P < 0.001$.

Lck-Cre transgene (40, 41). Floxing the *Ptpn2* allele did not in itself affect TCPTP expression (data not shown). TCPTP expression was ablated in *Lck*-Cre;*Ptpn2*$^{fl/fl}$ thymocytes (CD4$^+$CD8$^+$, CD4$^+$CD8$^-$, CD4$^-$CD8$^+$) and peripheral CD4$^+$ and CD8$^+$ T cells (as assessed by immunoblot analysis using two different mAbs specific to the N [3E2; data not shown] and C termini [6F3] of TCPTP), but not in splenic CD19$^+$ B cells, bone marrow–derived macrophages, or other tissues examined (data not shown, Figure 1C, and Supplemental Figure 1; supplemental material available online with this article; doi:10.1172/JCI59492DS1). At 4–12 weeks of age, *Lck*-Cre;*Ptpn2*$^{fl/fl}$ mice appeared normal and healthy (data not shown).

Thymocyte development in Lck-Cre;Ptpn2$^{fl/fl}$ *mice*. T cell progenitors develop in the thymus from double negative (DN; CD4$^-$CD8$^-$) to double positive (DP; CD4$^+$CD8$^+$) thymocytes and undergo selection and maturation, giving rise to CD4$^+$ and CD8$^+$ single positive (SP) thymocytes that emigrate to the periphery as mature T cells. At 4 weeks of age, *Lck*-Cre;*Ptpn2*$^{fl/fl}$ knockout mice had unaltered thymic cellularity and DP thymocyte numbers. However, CD4$^+$SP and CD8$^+$SP thymocytes (and CD4^{lo}CD8$^+$ and CD4$^+$CD8^{lo} SP intermediates) were significantly elevated, resulting in a 20% increase in the CD4$^+$SP/DP ratio and a 37.5% increase in the CD8$^+$SP/DP ratio (Figure 2A, Table 1, and Supplemental Fig-

Table 1
Thymocyte ratios in *Lck*-Cre;*Ptpn2*$^{fl/fl}$ mice

	CD4$^+$/CD8$^+$	CD8$^+$/DP	CD4$^+$/DP
Ptpn2$^{fl/fl}$ (n = 8)	4.02 ± 0.11	0.020 ± 0.001	0.08 ± 0.004
Lck-Cre;*Ptpn2*$^{fl/fl}$ (n = 8)	3.27 ± 0.09	0.032 ± 0.002	0.10 ± 0.006
P	0.0011	0.0002	0.01

Ptpn2$^{fl/fl}$ and *Lck*-Cre;*Ptpn2*$^{fl/fl}$ thymocytes from 4-week-old mice stained with fluorochrome-conjugated α-CD4 and -CD8 and analyzed by flow cytometry. Representative results (mean ± SEM) from 3 experiments are shown; significance was determined using 2-tailed Mann-Whitney *U* test.

ure 2A). No differences were noted in DP, SP, or SP/DP ratios in *Lck*-Cre;*Ptpn2*$^{fl/+}$ versus *Ptpn2*$^{fl/+}$ heterozygous mice (Supplemental Figure 3). The process of thymocyte positive selection can be minimally subdivided into 4 progressive stages based on changes in expression of TCRβ, CD69, and CD5 (42). Preselection DP cells (stage 1) are defined as TCRβ^{lo}, CD69^{lo}, and CD5^{lo}, whereas DP cells initiating positive selection (stage 2) are TCRβ$^{lo/int}$, CD69$^{int/hi}$, and CD5^{int}. Thymocytes in the process of positive selection (stage 3) are TCRβ$^{int/hi}$, CD69^{hi}, and CD5^{hi}, whereas SP cells that have completed positive selection (stage 4) are TCRβ^{hi}, CD5^{hi}, and CD69^{lo} (42). We noted significant increases in the number of *Lck*-Cre;*Ptpn2*$^{fl/fl}$ thymocytes that were undergoing (stage 3) or had completed (stage 4) positive selection (Figure 2B).

To further assess the impact of TCPTP deficiency on thymocyte development, we bred *Ptpn2*$^{fl/fl}$ and *Lck*-Cre;*Ptpn2*$^{fl/fl}$ mice onto OT-I and OT-II TCR transgenic backgrounds (43, 44). OT-II mice express a vα2/vβ5 TCR specific for the chicken OVA peptide ^{323}ISQAVHAAHAEINEAGR^{339} (presented in the context of I-A^b class II MHC), whereas OT-I mice express a vα2/vβ5 TCR that is specific for the OVA peptide ^{257}SIINEFKL^{264} (presented in the context of K^b class I MHC), selecting for CD4$^+$SP and CD8$^+$SP thymocytes, respectively (43, 44). Thymic cellularity in OT-II;*Lck*-Cre;*Ptpn2*$^{fl/fl}$ knockout mice was increased 2-fold when compared with littermate control OT-II;*Ptpn2*$^{fl/fl}$ mice (Figure 2C). This increase in cellularity was reflected by an increase in DP and CD4$^+$SP thymocytes. Importantly, whereas DP cells were increased by less than 2-fold, the increase in CD4$^+$SP thymocytes was more than 2-fold, translating into a significantly enhanced CD4$^+$SP/DP ratio (Figure 2C); similar increases were noted when only clonotypic vα2^{hi}vβ5^{hi} cells were assessed (Supplemental Figure 2B). Furthermore, the surface expression levels of TCRβ, CD69, and CD5 were increased in DP thymocytes (Supplemental Figure 2C), consistent with enhanced positive selection, and the numbers of thymocytes initiating (stage 2), undergoing (stage 3), and completing positive selection (stage 4) were also increased in OT-II *Lck*-Cre;*Ptpn2*$^{fl/fl}$ mice (Supplemental Figure 2D). In contrast, thymic cellularity and DP numbers were not altered in MHC class I–restricted OT-I *Lck*-Cre;*Ptpn2*$^{fl/fl}$ mice, but CD8$^+$SP thymocytes were increased, albeit modestly (Supplemental Figure 2E). Moreover, negative selection — as assessed by the deletion of TCRvβ5$^+$ CD4$^+$CD8$^-$ thymocytes by endogenous superantigen mouse mammary tumor virus 9 (MMTV9; which can be presented by I-A^b; refs. 45, 46) (Supplemental Figure 4A); the induction of the negative selection marker Nur77 (ref. 47 and Supplemental Figure 4B); and the induction of apoptosis in DP thymocytes in response to anti-CD3ε (Supplemental Figure 4C) — was altered modestly, if at all. Taken together, these results are consistent with TCPTP deficiency promoting thymocyte positive selection without compromising negative selection.

T cell subsets in Lck-Cre;Ptpn2$^{fl/fl}$ *mice*. In the LNs of 4- to 7-week-old *Lck*-Cre;*Ptpn2*$^{fl/fl}$ mice, the absolute numbers of CD4$^+$ and CD8$^+$ naive (CD62L^{hi}CD44^{lo}) T cells were increased (Figure 3 and Supplemental Figure 5), consistent with the elevated SP thymocyte development (Figure 2A). Naive T cells in spleen and liver were decreased in *Lck*-Cre;*Ptpn2*$^{fl/fl}$ mice, but this was accompanied by an increase in effector/memory (CD62L^{lo}CD44^{hi}) T cells (Figure 3 and Supplemental Figure 5). No difference was evident in the homing of *Lck*-Cre;*Ptpn2*$^{fl/fl}$ naive CD8$^+$ T cells to LN versus spleen after transfer into non-irradiated congenic Ly5.1 hosts (Supplemental Figure 6). The effector/memory phenotype in *Lck*-Cre;*Ptpn2*$^{fl/fl}$ mice was pronounced by 12 weeks of age, so that the total number of liver T cells was increased (Supplemental Figure 5). We found no overt differences in α-GalCer/CD1d tetramer$^+$/TCRβ$^+$ NKT cells, but moderate increases in CD4$^+$FoxP3$^+$CD25$^+$ regulatory T cells in thymus, LNs, and spleen, but not liver, in 7- to 12-week-old mice (Supplemental Figure 7). These findings suggest that TCPTP deficiency results in the accumulation of peripheral T cells with an effector/memory phenotype.

TCPTP regulates SFKs but not ZAP-70 in T cells. Previously, we reported that SFKs can serve as bona fide substrates for TCPTP and that TCPTP dephosphorylates the Y418 activation loop autophosphorylation site (corresponding to Y394 in Lck and Y417 in Fyn) to inactivate SFKs (48). Lck and Fyn are the predominant SFKs expressed in thymocytes and T cells and are essential for T cell development and function (2, 3). Accordingly, we assessed TCPTP's capacity to regulate T cell signaling by dephosphorylating and inactivating Lck and Fyn. As a first step, we determined whether Lck or Fyn could serve as TCPTP substrates. We took advantage of the TCPTP-D182A "substrate-trapping" mutant, which can form a stable complex with tyrosine phosphorylated substrates in a cellular context and protect such substrates from dephosphorylation by endogenous phosphatases (49–51). Human TCPTP or the TCPTP-D182A substrate-trapping mutant were coexpressed with wild-type Lck or the constitutively active Lck-Y505F mutant or with wild-type Fyn in COS1 cells, and phosphorylation of Lck and Fyn was monitored in cell lysates and TCPTP immunoprecipitates (Figure 4, A–C) using antibodies specific for Y418 phosphorylated SFKs. Expression of wild-type TCPTP ablated Lck and Fyn phosphorylation, whereas the TCPTP-D182A mutant enhanced Lck and Fyn phosphorylation, consistent with Lck and Fyn being direct substrates of TCPTP (Figure 4, A–C). As a control, we also assessed TCPTP's capacity to recognize the Syk family PTK ZAP-70 as a substrate (Figure 4D). ZAP-70 activation is dependent on Lck-mediated phosphorylation at Y493 (52). Accordingly, ZAP-70 was coexpressed with and without limiting amounts of activated Lck in COS1 cells. In the absence of Lck, ZAP-70 was minimally phosphorylated at Y493 by endogenous SFKs. Wild-type 45-kDa TCPTP readily suppressed ZAP-70 Y493 phosphorylation mediated by either endogenous SFKs or overexpressed Lck, whereas the TCPTP-D182A substrate-trapping mutant did not alter ZAP-70 phosphorylation, but readily increased the Y394 phosphorylation status of cotransfected Lck (Figure 4D). These results are consistent with TCPTP regulating ZAP-70 phosphorylation via Lck. The results indicate that TCPTP has the capacity to recognize SFKs such as Lck and Fyn, but not ZAP-70, as direct substrates.

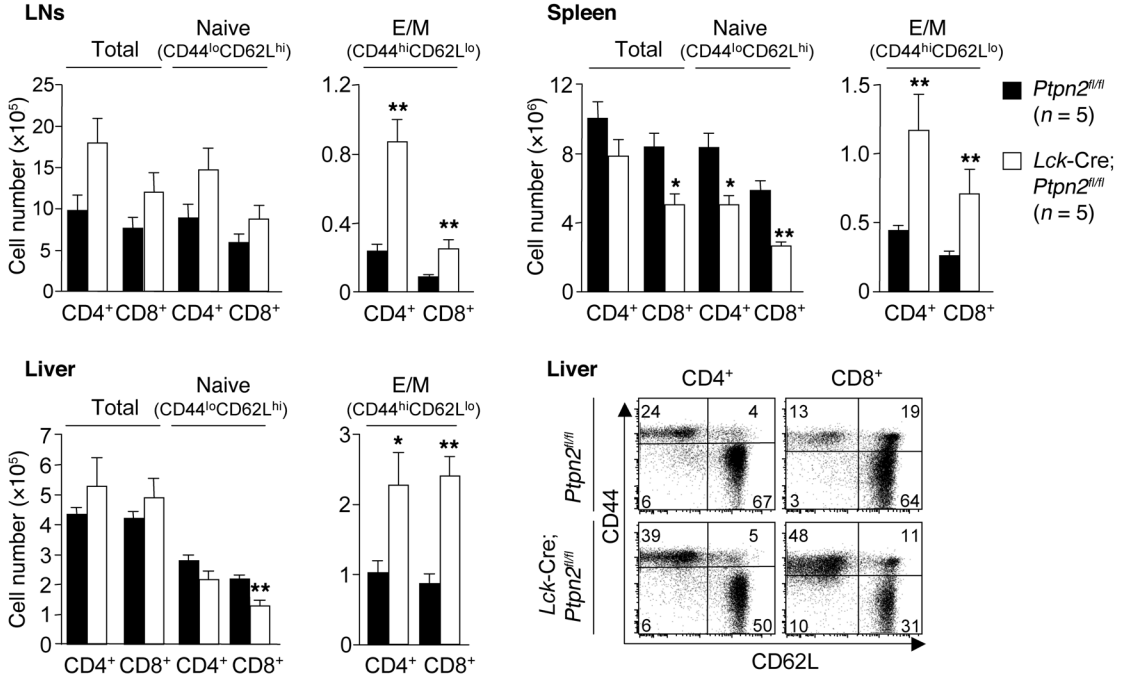

Figure 3

T cell subsets in *Lck-Cre;Ptpn2*$^{fl/fl}$ mice. *Ptpn2*$^{fl/fl}$ and *Lck*-Cre;*Ptpn2*$^{fl/fl}$ lymphocytes isolated from LNs, spleen, and liver of 7-week-old mice were stained with fluorochrome-conjugated antibodies against CD4, CD8, TCRβ, CD44, and CD62L and analyzed by flow cytometry. Absolute numbers of total CD4$^+$TCRβ$^+$ or CD8$^+$TCRβ$^+$ T cells and CD4$^+$ versus CD8$^+$ naive (CD44^{lo}CD62L^{hi}) and effector/memory-like (E/M) (CD44^{hi}CD62L^{lo}) T cells were determined. Representative dot plots (numbers in outlined areas are percentages of cells in gate) and results from 2 independent experiments are shown. Results shown are mean ± SEM for the indicated number of mice; significance was determined using 2-tailed Mann-Whitney *U* test; $^*P < 0.05$, $^{**}P < 0.01$.

Next we determined whether TCPTP could regulate SFKs in T cells. Overexpressed wild-type TCPTP (70% transfection efficiency) suppressed anti-CD3ε–induced SFK Y418 phosphorylation and downstream MAPK ERK1/2 signaling in Jurkat T cells (Figure 4E) and specifically suppressed SFK Y418 phosphorylation in Lck immunoprecipitates (Figure 4F). On the other hand, the TCPTP-D182A trapping mutant enhanced anti-CD3ε–induced SFK Y418 phosphorylation as assessed in cell lysates (Figure 4G) but did not enhance ZAP-70 phosphorylation (data not shown). These results indicate that TCPTP can attenuate TCR signaling by dephosphorylating and inactivating Lck and Fyn.

Ptpn2 deficiency enhances TCR signaling. To determine whether TCPTP regulates TCR signaling in vivo, we assessed the impact of TCPTP deficiency on SFK activation in thymocytes and T cells after crosslinking with CD3ε. For these studies, we focussed on purified CD8$^+$SP thymocytes and purified naive (CD44^{lo}) CD4$^+$ and CD8$^+$ LN T cells. Previous studies have shown that anti-CD3ε can activate both Fyn and Lck in T cells in vitro independent of coreceptor engagement (53, 54). Purified thymocytes and T cells were stimulated with anti-CD3ε, and SFK activation was assessed with SFK Y418 phosphorylation–specific antibodies that detect activated Fyn and Lck, or antibodies specific to the Y394 phosphorylation site in Lck. Basal SFK Y418 and Lck Y394 phosphorylation was not altered by TCPTP deficiency (Figure 5). In contrast, TCR-induced SFK Y418 phosphorylation was enhanced in *Lck*-Cre;*Ptpn2*$^{fl/fl}$ CD8$^+$SP thymocytes (Figure 5, A and B); enhanced SFK Y418 phosphorylation was seen in species comigrating with Lck and Fyn (Figure 5, A and B). In addition, Lck Y394 phosphorylation, as assessed with Y394 phosphorylation–specific antibodies in cell lysates or with SFK Y418 phosphorylation–specific antibodies in Lck immunoprecipitates, was also enhanced in *Lck*-Cre;*Ptpn2*$^{fl/fl}$ CD8$^+$SP thymocytes (Figure 5, C and D); enhanced Lck Y394 phosphorylation was particularly evident in Lck species with retarded electrophoretic mobility (Figure 5, C and D), previously associated with Lck activation (24, 55). Increased α-CD3–induced Lck Y394 phosphorylation and/or SFK Y418 phosphorylation were also evident in TCPTP-deficient naive CD8$^+$ T cells (Figure 4E and data not shown) and CD4$^+$ T cells (Supplemental Figure 8); no difference was evident in Lck Y505 phosphorylation in TCPTP-deficient naive CD8$^+$ T cells (Supplemental Figure 8). The elevated SFK activation correlated with increased tyrosine phosphorylation of specific proteins including Pyk2 and PLCγ1 (substrates of Fyn and ZAP-70, respectively) and elevated MAPK signaling as assessed by the phosphorylation of ERK1/2 (Figure 5A and Supplemental Figure 8). The enhanced α-CD3ε–induced signaling in SP thymocytes and T cells could not be ascribed to elevated CD3ε or TCRβ surface levels, or intracellular Lck, ZAP-70, PLCγ, LAT, or ERK2 (Supplemental Figure 9A). Indeed, TCRβ surface levels were reproducibly, albeit modestly, decreased in CD4$^+$ and CD8$^+$ naive T cells (Supplemental Figure 9B). Taken together, these results indicate that TCPTP deficiency enhances TCR signaling.

Deletion of Ptpn2 enhances TCR-dependent but not TCR-independent thymocyte proliferation. Our results indicate that TCPTP might be an important regulator of TCR-induced thymocyte signaling and responses. Accordingly, we assessed the impact of TCPTP deficiency on SP thymocyte proliferation. Proliferation was assessed

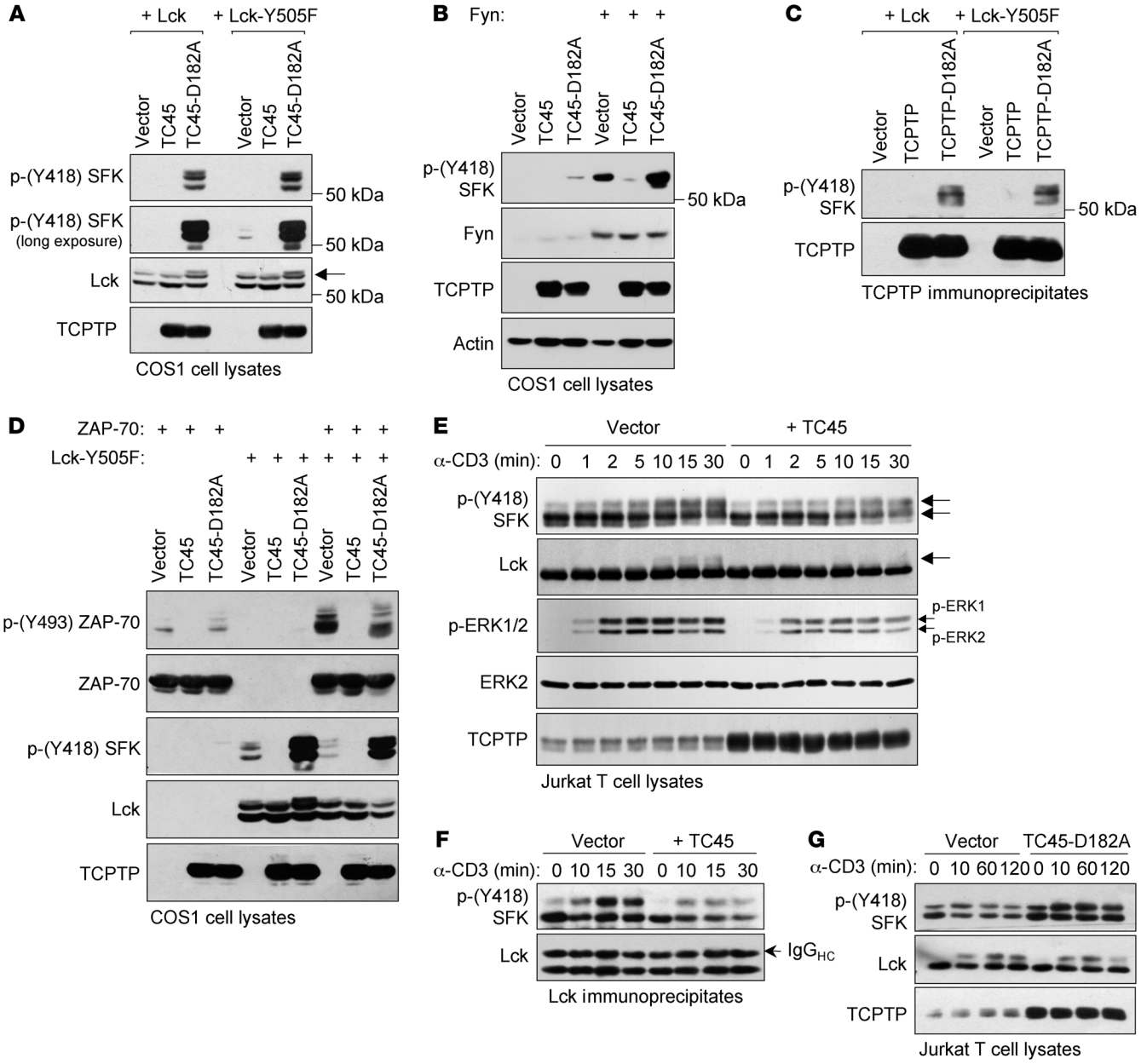

Figure 4

Lck and Fyn but not ZAP-70 can serve as TCPTP substrates. COS1 cells were transfected with vector control or constructs for 45-kDa TCPTP or TCPTP-D182A and (**A** and **C**) Lck or Lck-Y505F, (**B**) Fyn, or (**D**) ZAP-70. (**A**, **B**, and **D**) Cell lysates or (**C**) TCPTP immunoprecipitates were resolved by SDS-PAGE and immunoblotted for p-(Y418) SFK or p-(Y493) ZAP-70 and then reprobed as indicated. Lck species with retarded electrophoretic mobility resulting from TCPTP-D182A expression are indicated by arrows. (**E**–**G**) Jurkat E6.1 T cells transfected with vector control or constructs for TCPTP or TCPTP-D182A were stimulated by crosslinking with mouse α–human CD3ε at 37°C for the indicated times. (**E** and **G**) Cell lysates and (**F**) Lck immunoprecipitates were resolved by SDS-PAGE and immunoblotted for p-(Y418) SFK or antibodies specific for phosphorylated and activated ERK1/2 (p-ERK1/2) and reprobed as indicated. Retarded p-(Y418) SFK species indicative of Lck activation and p-ERK1 and p-ERK2 as well as the IgG heavy chain (IgG$_{HC}$) are highlighted by arrows. Results shown are representative of 3 independent experiments.

in *Ptpn2*$^{fl/fl}$ versus *Lck*-Cre;*Ptpn2*$^{fl/fl}$ SP thymocytes in response to either TCR crosslinking with anti-CD3ε with/without anti-CD28, or stimulating with the phorbol ester PMA plus the calcium ionophore ionomycin, to promote TCR-dependent and -independent proliferation, respectively. TCPTP deficiency resulted in increased anti-CD3ε–induced thymocyte proliferation as monitored by [^{3}H]thymidine incorporation (Figure 6A and Supplemental Figure 10A). The increased proliferation seen in response to anti-CD3ε stimulation alone in *Lck*-Cre;*Ptpn2*$^{fl/fl}$ thymocytes was similar to that achieved with anti-CD3ε plus anti-CD28 in *Ptpn2*$^{fl/fl}$ cells. Enhanced proliferation was observed in both CD8$^+$SP and CD4$^+$SP thymocytes as assessed by the dilution of CFSE, which

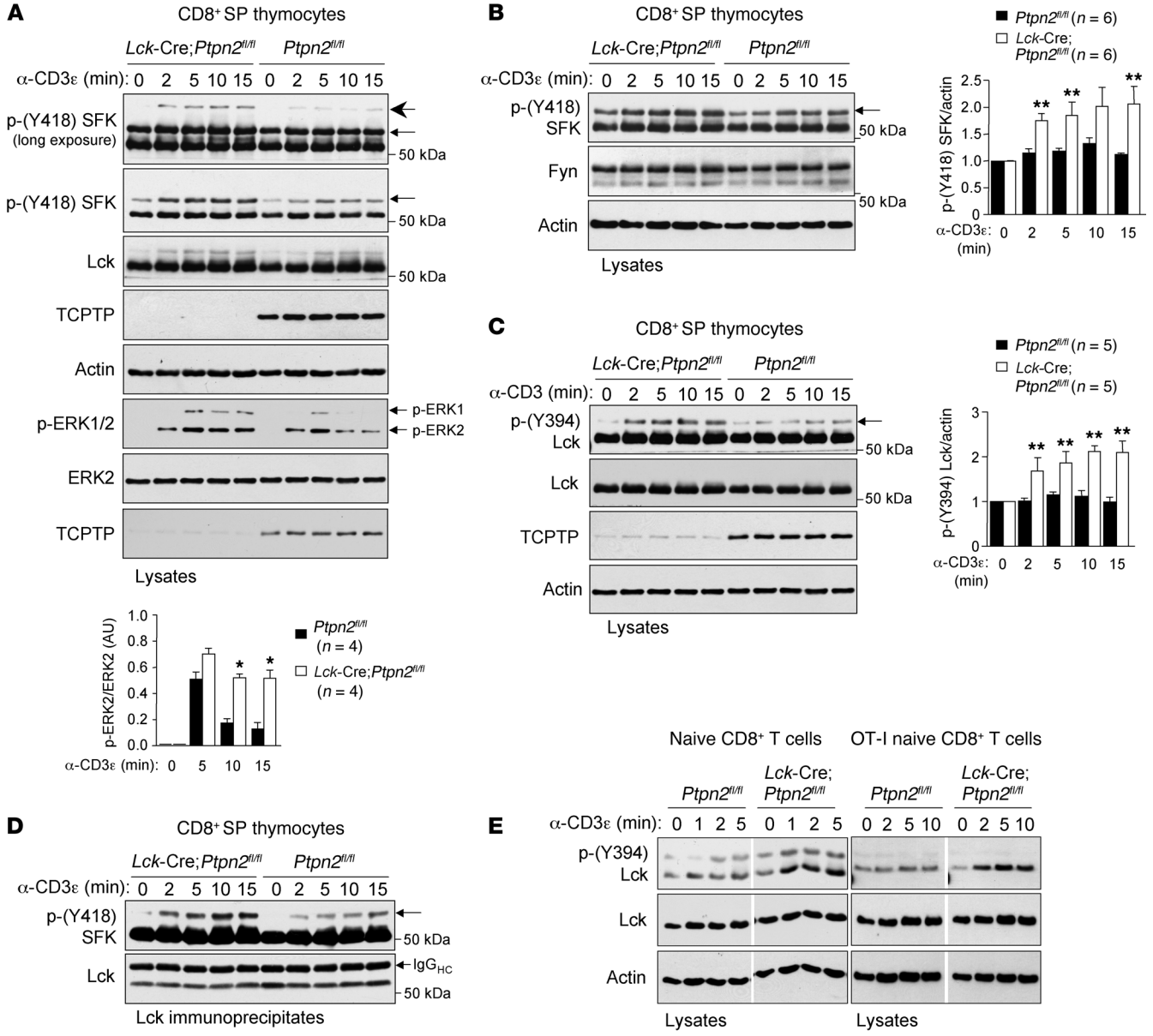

Figure 5

Ptpn2 deletion enhances TCR signaling. (**A**–**D**) MACS-purified (Miltenyi Biotec) CD8+SP thymocytes or (**E**) FACS-purified LN naive (CD44lo) CD8+ T cells or OT-I LN naive CD8+ T cells from *Ptpn2*$^{fl/fl}$ and *Lck*-Cre;*Ptpn2*$^{fl/fl}$ mice were stimulated with α-CD3ε at 37°C for the indicated times. Cell lysates or Lck immunoprecipitates were resolved by SDS-PAGE and immunoblotted for p-(Y418) SFK, p-(Y394) Lck, or p-ERK1/2 and then reprobed with actin as indicated. Retarded p-(Y418) SFK and p-(Y394) Lck species and p-ERK1 and p-ERK2 as well as IgG_{HC} are indicated by arrows. Results shown are representative of at least 3 independent experiments. In **A**–**C**, electrophoretically retarded p-(Y418) SFK and p-(Y394) Lck species and p-ERK2 were quantified by densitometric analysis and normalized for actin or ERK2 as indicated. In **A**, data are shown as arbitrary units (AU). Quantified results are mean ± SEM for the indicated number of independent experiments; significance was determined using 2-tailed Mann-Whitney *U* test; **P* < 0.05, ***P* < 0.01.

measures division on a per-cell basis (Supplemental Figure 10B). In contrast, proliferation induced by PMA/ionomycin was not increased in *Lck*-Cre;*Ptpn2*$^{fl/fl}$ versus *Ptpn2*$^{fl/fl}$ thymocytes (Figure 6A). Thus, the increased proliferative capacity of TCPTP-deficient thymocytes may be specific to that induced by the TCR. Increased anti-CD3ε– but not PMA/ionomycin-induced proliferation was also evident in sorted CD8+SP *Lck*-Cre;*Ptpn2*$^{fl/fl}$ thymocytes (Figure 6A) and in sorted CD8+SP and CD4+SP thymocytes from 14-day-old *Ptpn2*$^{-/-}$ mice (ref. 38 and Supplemental Figure 10C). There was no overt difference in the proliferation of CD8+SP thymocytes from *Lck*-Cre;*Ptpn2*$^{fl/+}$ heterozygous mice (Figure 6A). These results indicate that homozygous TCPTP deficiency enhances TCR-dependent, but not -independent, SP thymocyte proliferation.

Deletion of Ptpn2 enhances T cell activation and proliferation in vitro. Since TCPTP deficiency increased TCR signaling, we next determined the impact of TCPTP deficiency on T cell activation and

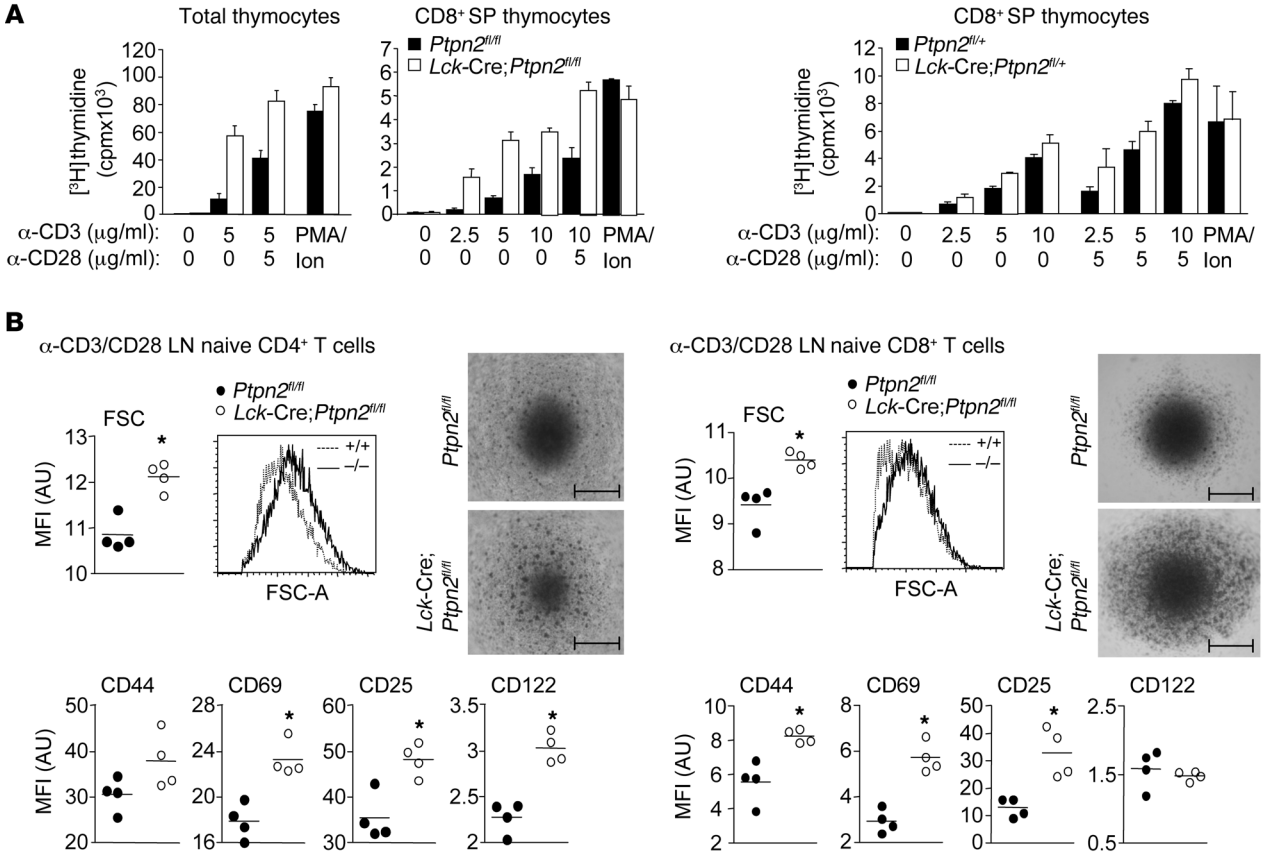

Figure 6

Ptpn2 deletion enhances thymocyte proliferation and T cell activation in vitro. (**A**) *Ptpn2*$^{fl/fl}$ and *Lck*-Cre;*Ptpn2*$^{fl/fl}$ total thymocytes or FACS-purified *Ptpn2*$^{fl/fl}$ and *Lck*-Cre;*Ptpn2*$^{fl/fl}$ or *Ptpn2*$^{fl/+}$ and *Lck*-Cre;*Ptpn2*$^{fl/+}$ CD8+SP thymocytes from 4-week-old mice were stimulated with plate-bound α-CD3ε with or without α-CD28 or PMA (1 ng/ml) plus ionomycin (Ion; 200 ng/ml), and proliferation was determined by [^{3}H]thymidine incorporation. Results are mean ± SD from quadruplicate determinations and are representative of at least 3 independent experiments. (**B**) FACS-purified CD4+ naive (CD25^{lo}CD44^{lo}CD62^{hi}) or CD8+ (CD44^{lo}CD62^{hi}) LN T cells (2×10^5) from 4-week-old *Ptpn2*$^{fl/fl}$ and *Lck*-Cre;*Ptpn2*$^{fl/fl}$ mice were stimulated with plate-bound α-CD3ε (5 μg/ml) and α-CD28 (2.5 μg/ml) for 48 hours. Photographs were taken and cells harvested and stained with fluorochrome-conjugated antibodies against CD44, CD69, CD25, and CD122. Cells were analyzed by flow cytometry and the indicated MFI determined; data are shown as arbitrary units (AU), and significance was determined using 2-tailed Mann-Whitney *U* test; $^*P < 0.05$. Representative photographs, forward scatter (FSC) plots, and results from 2 independent experiments are shown. Scale bars: 1 mm.

proliferation. First, we assessed the activation of CD4+ and CD8+ naive LN T cells in response to α-CD3/α-CD28 by monitoring blast formation by flow cytometry (monitoring cell size) and light microscopy and the cell surface expression levels of CD44, CD69, and the IL-2 receptor α (CD25) and β (CD122) subunits (Figure 6B). We found that blast formation was increased in both CD4+ and CD8+ TCPTP-deficient T cells after 48 hours stimulation. In addition, CD44, CD69, CD25, and CD122 levels were increased in CD4+ T cells, and CD44, CD69, and CD25 levels were elevated in CD8+ TCPTP-deficient T cells following α-CD3/α-CD28 stimulation. Consistent with the elevated IL-2 receptor (CD25/CD122) expression, we found that IL-2–induced STAT5 Y694 phosphorylation and T cell proliferation were enhanced in TCPTP-deficient T cells (Supplemental Figure 11, A and B). In contrast, IL-4–induced STAT6 Y641 phosphorylation and cell proliferation were not altered by TCPTP deficiency (Supplemental Figure 12). Second, we determined the impact of TCPTP deficiency on naive CD4+ and CD8+ T cell proliferation in response to varying amounts of plate-bound anti-CD3ε (Figure 7A). TCPTP homozygous deficiency significantly enhanced the anti-CD3ε–induced proliferation (as assessed by CFSE dilution) of purified LN naive (CD44^{lo}) CD8+ T cells (Figure 7A). Importantly, we noted that *Lck*-Cre;*Ptpn2*$^{fl/fl}$ CD8+ T cells readily proliferated at anti-CD3ε concentrations that were largely ineffective in promoting wild-type *Ptpn2*$^{fl/fl}$ T cell proliferation, approximating that seen in response to anti-CD3ε plus anti-CD28 in *Ptpn2*$^{fl/fl}$ cells. These results are consistent with TCPTP deficiency both lowering the threshold for TCR-induced proliferation and reducing the need for co-stimulation. No significant differences were evident in naive CD8+ T cells from *Lck*-Cre;*Ptpn2*$^{fl/+}$ versus *Ptpn2*$^{fl/+}$ heterozygous mice (Supplemental Figure 10D), in line with the enhanced proliferation being due to TCPTP deficiency, rather than *Lck*-Cre. Threshold responses (as assessed by CFSE dilution) were not altered in naive CD4+ (CD25^{lo}CD44^{lo}CD62L^{hi}) T cells (Figure 7B), but CD4+ T cell proliferation, as assessed by [^{3}H]thymidine incorporation, was increased approximately 2-fold (Figure 7C). This is in keeping with the elevated anti-CD3ε–induced IL-2 receptor expression and IL-2–induced signaling in CD4+ T cells (Figure 6B and

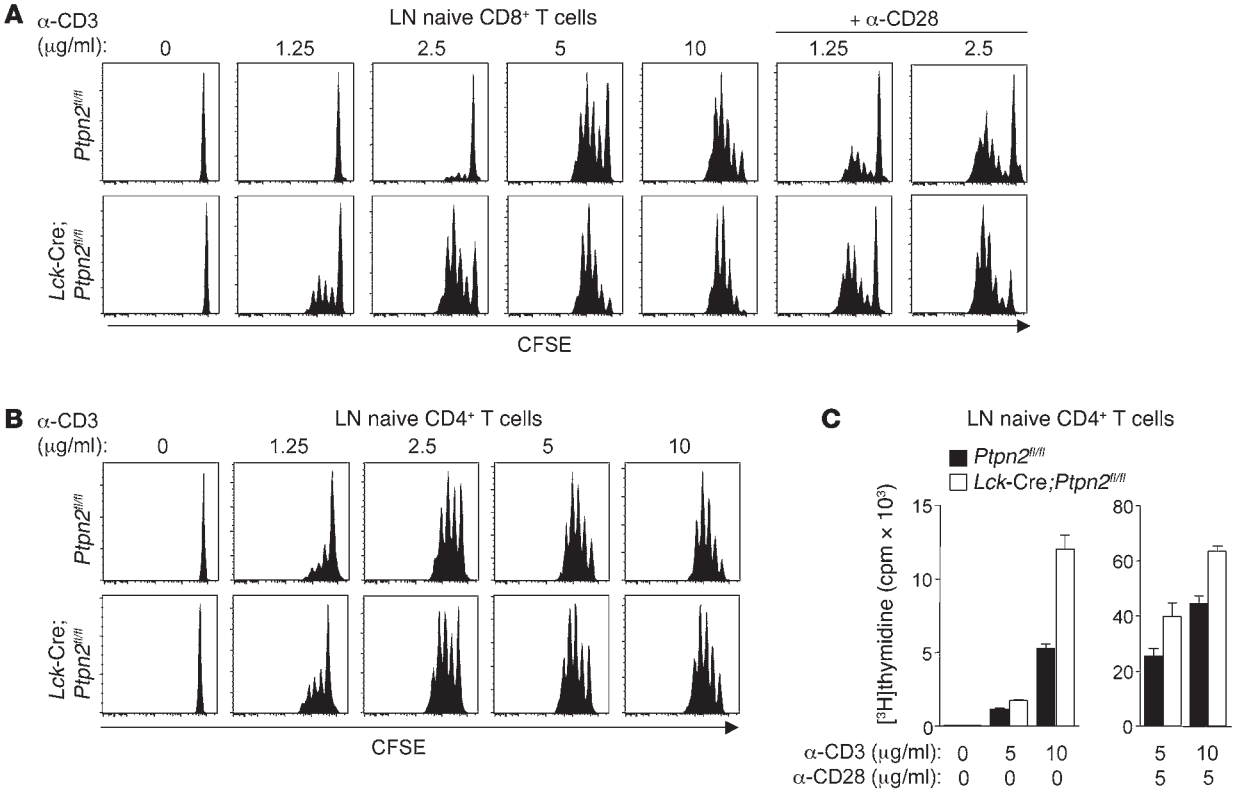

Figure 7

Ptpn2 deletion enhances T cell proliferation in vitro. (**A** and **B**) FACS-purified CD8+ (CD44lo) or CD4+ naive (CD25loCD44lo) LN T cells from 4-week-old *Ptpn2*$^{fl/fl}$ and *Lck*-Cre;*Ptpn2*$^{fl/fl}$ mice were stained with CFSE and stimulated with plate-bound α-CD3ε with or without α-CD28 (2.5 μg/ml) for 72 hours. Representative profiles from 3 independent experiments are shown. (**C**) FACS-purified *Ptpn2*$^{fl/fl}$ and *Lck*-Cre;*Ptpn2*$^{fl/fl}$ CD4+ naive (CD25loCD44lo) LN T cells from 4-week-old mice were stimulated with plate-bound α-CD3ε with or without α-CD28 for 48 hours, and proliferation was determined by [3H]thymidine incorporation. Results are mean ± SD from triplicate determinations and are representative of 3 independent experiments.

Supplemental Figure 11A). Taken together, these results indicate that TCPTP homozygous deficiency enhances TCR-induced CD4+ and CD8+ T cell activation and T cell proliferation.

Deletion of Ptpn2 enhances antigen-induced CD4+ and CD8+ T cell responses in vivo. To examine TCPTP's role in TCR-induced T cell responses in vivo, we compared the proliferation of CFSE-labeled *Ptpn2*$^{fl/fl}$ and *Lck*-Cre;*Ptpn2*$^{fl/fl}$ OT-I CD8+ or OT-II CD4+ naive (CD44lo) T cells that had been adoptively transferred into non-irradiated syngeneic mice and challenged with cognate peptide antigen SIINFEKEL (N4; Figure 8A) or OVA (Figure 8B), respectively. Antigen-induced proliferation, as assessed by CFSE dilution, was reproducibly and significantly increased in *Lck*-Cre;*Ptpn2*$^{fl/fl}$ OT-I CD8+ and OT-II CD4+ T cells isolated from LNs, spleen, and liver (Figure 7, A and B, and data not shown). Therefore, these results provide evidence for TCPTP deficiency enhancing TCR-induced T cell responses in vivo.

Ptpn2 deletion enhances CD8+ T cell responses to low-affinity antigens. Our findings indicate that TCPTP deficiency enhances TCR-instigated T cell activation and proliferation in vitro and in vivo. Moreover, our results suggest that TCPTP deficiency may permit CD8+ T cells to respond to antigen that may otherwise not be of high enough affinity to promote cellular division. A key advantage of the OT-I system is the availability of altered peptide ligands (APLs) based on N4 (Y3, Q4) for which TCR affinities and/or lytic or IFN-γ responses have been established (N4 > Y3 > Q4) (11, 14, 56). Accordingly, we compared the proliferation of *Ptpn2*$^{fl/fl}$ versus *Lck*-Cre;*Ptpn2*$^{fl/fl}$ naive OT-I CD8+ T cells stimulated with N4 versus APLs with lower TCR affinity. As a first step, we compared the proliferation of purified *Ptpn2*$^{fl/fl}$ versus *Lck*-Cre;*Ptpn2*$^{fl/fl}$ naive OT-I CD8 T cells in vitro in response to N4 versus Y3 and Q4 (Figure 9A). Since previous studies have established that responses induced by peptide presented by anchored class I MHC can be ascribed predominantly to eluted peptide self-presented by T cells (57, 58), we added peptides directly to the culture supernatant. Hommel et al. (58) have established that both TCR affinity and peptide antigen concentration dictate the response time, with lower affinity and concentration prolonging the time to first division. Therefore, we determined the impact of TCPTP deficiency on cell division by monitoring the dilution of CFSE to varying concentrations of N4, Y3, and Q4. TCPTP deficiency enhanced the responses to N4, Y3, and Q4, promoting cell division in a concentration-dependent manner. Importantly, the effects on cell division correlated with peptide affinity/responsiveness, with greater differences seen for Y3 and Q4 than N4 (Figure 9A).

Next, we determined whether TCPTP deficiency lowers the threshold for TCR-mediated proliferation in vivo. Previous studies have established that 4-fold-higher amounts of Y3 versus N4 are needed to induce a half-maximal IFN-γ response in OT-I T cells (14). Accordingly, we compared the proliferation of *Ptpn2*$^{fl/fl}$ and *Lck*-Cre;*Ptpn2*$^{fl/fl}$ adoptively transferred CFSE-labeled naive

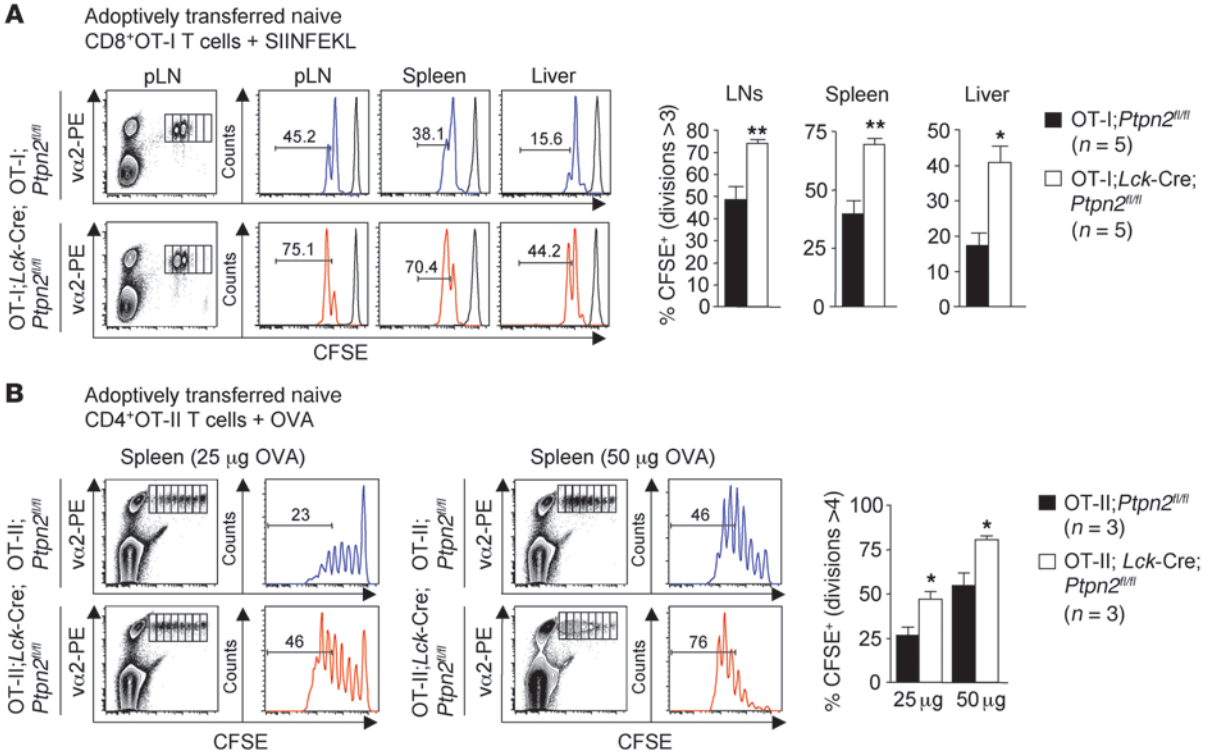

Figure 8

Ptpn2 deletion enhances T cell proliferation in vivo. (**A**) FACS-purified CD8+ naive LN T cells from 4-week-old OT-I;*Ptpn2*$^{fl/fl}$ and OT-I;*Lck*-Cre;*Ptpn2*$^{fl/fl}$ mice were stained with CFSE and transferred into syngeneic hosts, which were immunized 24 hours later with vehicle control (PBS) or 2.5 μg SIINFEKL. Forty-eight hours after immunization LN, splenic, and liver T cells were isolated and stained with fluorochrome-conjugated antibodies against CD8 and TCRvα2 and CD8+ T cells analyzed by flow cytometry. Representative profiles (numbers are percentages of cells that have undergone >3 divisions) are shown; PBS controls are shown in black. Quantified results are mean ± SEM (pooled cells from 2 donors transferred into 5 recipients in each case) and are representative of 3 independent experiments; significance was determined using 2-tailed Mann-Whitney *U* test; **P* < 0.05, ***P* < 0.01. (**B**) FACS-purified CD4+ naive LN T cells from 4 -week-old OT-II;*Ptpn2*$^{fl/fl}$ and OT-II;*Lck*-Cre;*Ptpn2*$^{fl/fl}$ mice were stained with CFSE and transferred into syngeneic hosts and 24 hours later immunized with OVA. Seventy-two hours after immunization, splenic T cells were isolated and stained with fluorochrome-conjugated antibodies against CD4 and TCRvα2 and CD4+ T cells analyzed by flow cytometry. Representative profiles (numbers are percentages of cells that have undergone >4 divisions) are shown. Quantified results are mean ± SEM (cells from 3 donors transferred into 2 recipients in each case and stimulated with 25 or 50 μg OVA) and are representative of 3 independent experiments; significance was determined using a 2-tailed Student's *t* test; **P* < 0.05.

OT-I CD8+ T cells 3 days after injection of N4 versus Y3 (Figure 9B). In these experiments, naive OT-I CD8+ CFSE-labeled donor T cells from each mouse were transferred into two hosts and subsequently injected with N4 versus Y3, allowing for direct comparisons of responses. Only modest increases in proliferation were noted for N4 in *Lck*-Cre;*Ptpn2*$^{fl/fl}$ versus *Ptpn2*$^{fl/fl}$ transferred OT-I T cells 3 days after peptide administration (compare Figure 8A, where proliferation was assessed 2 days after peptide administration). In contrast, TCPTP deficiency significantly enhanced the proliferation of *Lck*-Cre;*Ptpn2*$^{fl/fl}$ OT-I T cells stimulated with Y3 (Figure 9B). Taken together, these findings are consistent with TCPTP deficiency lowering the threshold for TCR-instigated proliferation in vivo and allowing CD8+ T cells to respond to peptides with suboptimal TCR affinity.

Inflammation and autoimmunity in Lck-Cre;Ptpn2$^{fl/fl}$ *mice.* One possible consequence of lowering the threshold for TCR-induced responses in *Lck*-Cre;*Ptpn2*$^{fl/fl}$ mice could be the development of immune and inflammatory disorders. We found that in 48-week-old aged *Lck*-Cre;*Ptpn2*$^{fl/fl}$ mice, circulating levels of the proinflammatory cytokines IL-6, TNF, and IFN-γ, as well as chemokines MIG and RANTES, previously associated with intrahepatic inflammation (59), were significantly elevated (Figure 10A). Furthermore, consistent with the development of inflammation, we found significant increases in CD4+ and CD8+ CD44^{hi}CD62L^{lo} effector/memory T cells in *Lck*-Cre;*Ptpn2*$^{fl/fl}$ LNs (resulting in increased LN weights; Supplemental Figure 13) and bone marrow, as well as lymphocytic infiltrates in non-lymphoid tissues such as liver and lung, associated with striking increases in CD44^{hi}CD62L^{lo} T cells (Figure 10, B, D, and E). Importantly, CD8+CD44^{hi}CD62L^{lo} T cells in the livers of aged mice were high for KLRG1 and low for CD127 (IL-7Rα) (Figure 10C), consistent with these being activated CD8+ effector T cells (60). In addition, TCPTP deficiency resulted in peanut agglutinin–positive germinal centers in the spleens of aged mice (Supplemental Figure 14) and high levels of anti-nuclear antibodies in sera (Figure 11A), indicative of a breakdown in tolerance. Indeed, aged *Lck*-Cre;*Ptpn2*$^{fl/fl}$ mice had significantly reduced body weights (Figure 11B), and 2 of 5 mice exhibited dermatitis and had to be culled by 10 months of age (data not shown). Moreover, hepatic

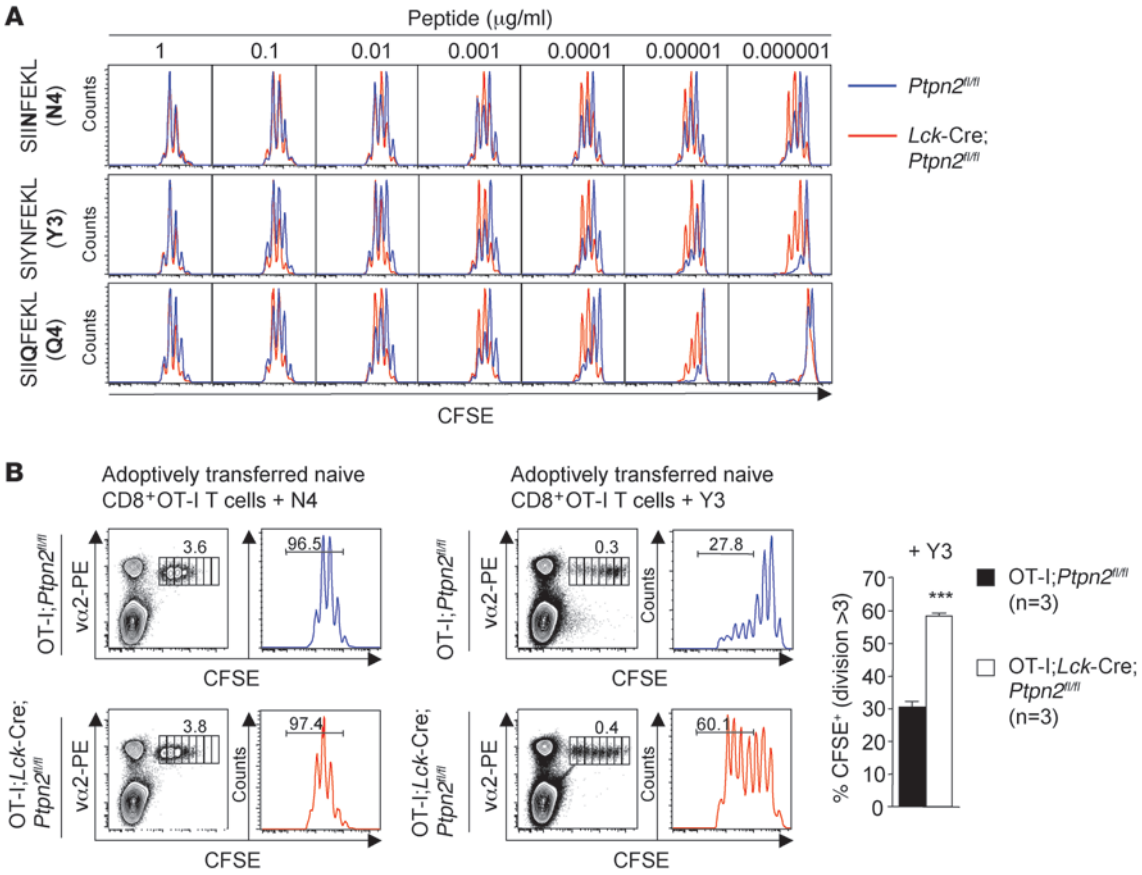

Figure 9

Ptpn2 deletion lowers the threshold for CD8+ T cell proliferation. (**A**) FACS-purified CD8+ naive LN T cells from 4-week-old OT-I;*Ptpn2*$^{fl/fl}$ and OT-I;*Lck*-Cre;*Ptpn2*$^{fl/fl}$ mice were stained with CFSE and incubated with the indicated concentrations of SIINFEKL (N4), SIYNFEKL (Y3), or SIIQFEKL (Q4) for 48 hours and analyzed by flow cytometry. Representative profiles from 3 independent experiments are shown. (**B**) FACS-purified CD8+ naive LN T cells from 4-week-old OT-I;*Ptpn2*$^{fl/fl}$ and OT-I;*Lck*-Cre;*Ptpn2*$^{fl/fl}$ mice were stained with CFSE and transferred into syngeneic hosts and immunized with 1.25 μg N4 or Y3. At 72 hours after immunization, peripheral LN T cells were isolated and stained with fluorochrome-conjugated antibodies against CD8 and TCRvα2 and CD8+ T cells analyzed by flow cytometry. Representative dot plots (numbers are percentages of cells in gate), CFSE profiles (numbers are percentages of cells that have undergone >3 divisions), and quantified results are shown. Quantified results are mean ± SEM (from 3 donors transferred into 2 recipients in each case and stimulated with N4 versus Y3) and are representative of at least 3 independent experiments; significance was determined using 2-tailed Student's *t* test; ***$P < 0.001$.

lymphocytic infiltrates were accompanied by the development of fibrosis (assessed by staining with sirius red; Figure 11C) and overt liver damage as assessed by the presence of the hepatic enzymes alanine transaminase (ALT) and aspartate amino transferase (AST) in serum (Figure 11D). TCPTP expression was not altered in B220+ LN B cells, in splenic macrophages (Ly6G$^{-/lo}$CD11B+), granulocytes (Ly6G^{hi}CD11B+) and dendritic cells (CD11c+) (Supplemental Figure 15), or in other tissues (data not shown) of aged *Lck*-Cre;*Ptpn2*$^{fl/fl}$ mice, consistent with the disease being a consequence of TCPTP deletion in T cells. Moreover, TCPTP deficiency did not alter the anti-CD3ε/IL-2–induced proliferation of regulatory T cells (CD4+CD25^{hi}), nor did it affect their capacity to suppress the proliferation of naive (CD44^{lo}CD25^{lo}) CD4+ T cells in response to anti-CD3ε (Supplemental Figure 16). Therefore, these results indicate that the development of disease in aged *Lck*-Cre;*Ptpn2*$^{fl/fl}$ mice could not be attributed to a defect in regulatory T cell function. Nonetheless, we performed additional experiments to establish whether the disease in *Lck*-Cre;*Ptpn2*$^{fl/fl}$ mice was T cell intrinsic/dependent. Total CD8+ T cells from the spleens of aged *Ptpn2*$^{fl/fl}$ and *Lck*-Cre;*Ptpn2*$^{fl/fl}$ mice (Supplemental Figure 17) were transferred into sublethally irradiated congenic hosts, and 12 weeks later, organ damage and serum anti-nuclear antibodies were assessed (Figure 11E and Supplemental Figure 17). We found that CD8+ T cells from *Lck*-Cre;*Ptpn2*$^{fl/fl}$ mice resulted in a significant increase in anti-nuclear antibodies and liver damage as monitored by the presence of serum ALT and AST (Figure 11E). Taken together, these results indicate that TCPTP deficiency in T cells results in a breakdown in tolerance and the development of autoimmunity.

Discussion

TCR signaling affects the selection and survival of T cells at every stage of development (2, 3). In keeping with TCPTP being a key negative regulator of TCR signaling, we found that CD8+SP and CD4+SP thymocyte numbers were increased in *Lck*-Cre;*Ptpn2*$^{fl/fl}$ mice. In contrast, mice deficient for the phosphatases SHP-1 or PEP, which have been implicated in Lck dephosphorylation

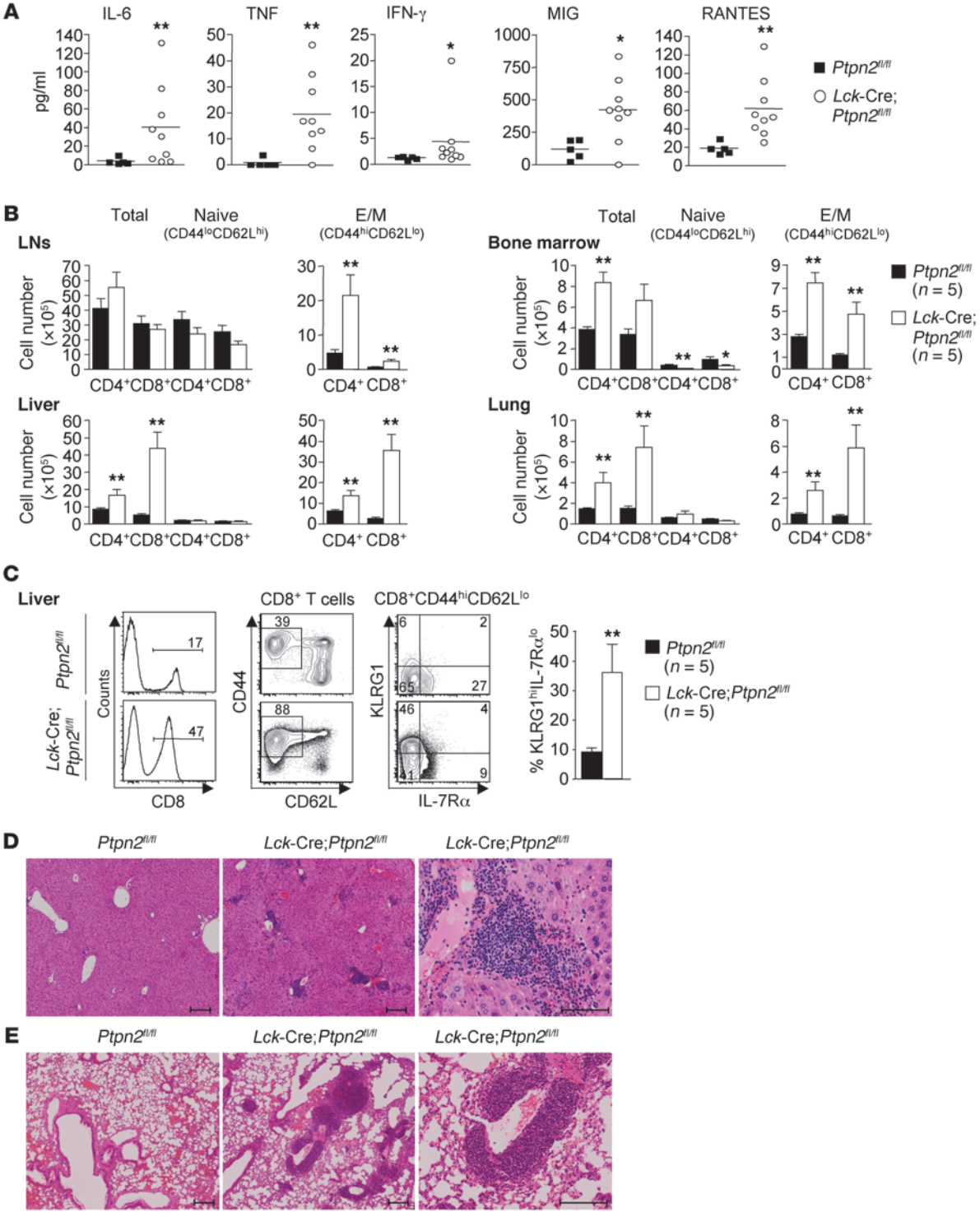

Figure 10

Inflammation and lymphocytic infiltrates in *Lck*-Cre;*Ptpn2*$^{fl/fl}$ mice. (**A**) Cytokine levels in serum from 48-week-old *Ptpn2*$^{fl/fl}$ and *Lck*-Cre;*Ptpn2*$^{fl/fl}$ mice were determined by flow cytometry using a BD Cytokine Bead Array (BD Biosciences). (**B** and **C**) *Ptpn2*$^{fl/fl}$ and *Lck*-Cre;*Ptpn2*$^{fl/fl}$ lymphocytes (3×10^6) isolated from LNs, bone marrow, liver, and lung of 40-week-old mice were stained with fluorochrome-conjugated antibodies against CD4, CD8, CD44, CD62L, KLRG1, and IL-7Rα and analyzed by flow cytometry. (**B**) Absolute numbers of total CD4$^+$ or CD8$^+$ T cells and CD4$^+$ versus CD8$^+$ naive (CD44^{lo}CD62L^{hi}) and effector/memory-like (CD44^{hi}CD62L^{lo}) T cells were determined. (**C**) The relative numbers of KLRG1^{hi}IL-7Rα^{lo} CD8$^+$ effector/memory T cells (CD44^{hi}CD62L^{lo}) and representative FACS plots are shown. Formalin-fixed (**D**) liver sections from 48-week-old mice or (**E**) lung sections from 40-week-old mice were stained with hematoxylin and eosin. Representative images are shown from 2 independent experiments. Scale bars: 200 μM, low magnification; 100 μM, high magnification. Results shown in **A**–**C** are mean ± SEM for the indicated number of mice and are representative of at least 2 independent experiments; significance was determined using 2-tailed Mann-Whitney *U* test; $^*P < 0.05$, $^{**}P < 0.01$.

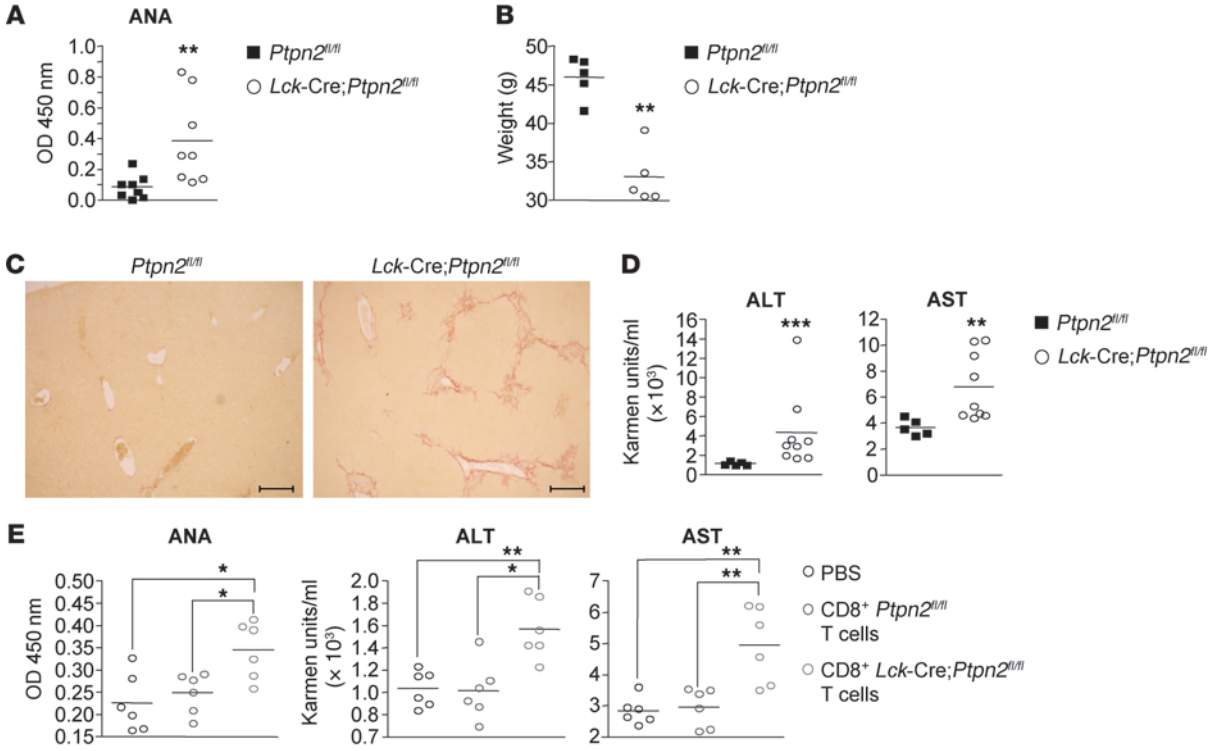

Figure 11

ANAs and organ damage in *Lck*-Cre;*Ptpn2*$^{fl/fl}$ mice. (**A**) Serum ANAs in 40-week-old *Ptpn2*$^{fl/fl}$ and *Lck*-Cre;*Ptpn2*$^{fl/fl}$ mice were measured using a mouse ANA Ig's (total IgA+G+M) ELISA Kit. (**B**) Body weights of 40-week-old *Ptpn2*$^{fl/fl}$ and *Lck*-Cre;*Ptpn2*$^{fl/fl}$ mice. (**C**) Formalin-fixed liver sections from 48-week-old mice were stained with picrosirius red. Representative images are shown. Scale bars: 200 μM. (**D**) Serum ALT and AST activities in 48-week-old *Ptpn2*$^{fl/fl}$ and *Lck*-Cre;*Ptpn2*$^{fl/fl}$ mice were determined using a Transaminase CII kit. (**E**) PBS or FACS-purified CD8$^+$ lymphocytes isolated from the spleens of aged *Ptpn2*$^{fl/fl}$ and *Lck*-Cre;*Ptpn2*$^{fl/fl}$ mice were transferred (2×10^6/recipient) into sublethally irradiated (600 rad) congenic Ly5.1 hosts. Twelve weeks after transfer, serum ANAs were measured, and serum ALT and AST activities were determined. Results shown are means for the indicated number of mice; significance was determined using 2-tailed Mann-Whitney *U* test; $^*P < 0.05$, $^{**}P < 0.01$, $^{***}P < 0.001$.

and inactivation, do not have any overt alterations in thymocyte subsets, unless placed on TCR transgenic backgrounds (29, 61). PEP-knockout mice on MHC class I– or II–restricted TCR transgenic backgrounds have enhanced positive but unaltered negative selection (29), whereas SHP-1 mutant (*motheaten/motheaten*) mice exhibit a dramatic decrease in DP numbers and a relative increase in CD4$^+$SP thymocytes on an MHC class II–restricted TCR transgenic background, consistent with elevated negative and positive selection (61). In our studies, TCPTP deficiency increased positive selection but did not appear to alter negative selection. Importantly, TCPTP deficiency enhanced naive T cell responses to low-affinity ligands. Therefore, the selective effects of TCPTP deficiency on positive selection may be attributable to the enhanced responsivity of a subset of thymocytes with low affinity for self-pMHC. Similarly, differences in OT-I versus OT-II thymocyte responses to self-pMHC may be responsible for the contrasting effects of TCPTP deficiency on OT-I versus OT-II thymocyte development. However, we cannot exclude the possibility that additional pathways may be altered in *Lck*-Cre;*Ptpn2*$^{fl/fl}$ mice to affect thymocyte development. T cell–specific SOCS-1–deficient mice have increased CD8$^+$SP, but not CD4$^+$SP, thymocytes due to elevated IL-7–induced STAT5 signaling in DP thymocytes (62). STAT5 can serve as a TCPTP substrate (63, 64), and IL-2–induced STAT5 phosphorylation is increased in LN T cells from *Ptpn2*$^{-/-}$ mice that are globally deficient for TCPTP (64). It is possible that elevated cytokine signaling may have in part contributed to the effects of TCPTP deficiency on CD8$^+$SP thymocyte development. On the other hand, the increased CD4$^+$SP thymocyte development may have been due to elevated TCR signaling alone, since high levels of SFK activation favor the development of CD4$^+$SP thymocytes (65, 66).

In the periphery, TCPTP deficiency resulted in a memory phenotype. The number of T cells with an effector/memory phenotype increased progressively from 4 to 12 weeks of age, and this was accompanied by a decrease in naive T cell numbers. Early in life, the peripheral T cell pool consists largely of naive T cells, but with age and thymic atrophy, this shifts to a predominance of memory T cells (67). Memory T cells are generated after an immune challenge and the exposure of naive T cells to foreign antigen. However, naive T cell homeostasis and lymphopenia-induced proliferation (LIP) can also result in the generation of "memory phenotype" cells, and these cells have many of the characteristics of true memory T cells (67). The generation of memory phenotype T cells is dependent on naive T cell TCR interaction with low-affinity self-pMHC plus interaction with γ_c cytokines (67). The rate of naive T cell LIP relies on TCR affinity for self-pMHC; T cells with high-affinity TCRs proliferate faster than T cells with low-affinity TCRs (68, 69). Thus, an overall consequence of LIP is the selection of high-affinity, potentially self-

reactive T cells. One possibility is that the memory phenotype and the decline in the naive T cell pool in *Lck*-Cre;*Ptpn2*$^{fl/fl}$ mice may have been attributable to the conversion of naive T cells to memory phenotype T cells due to enhanced T cell homeostasis/LIP. Moreover, by lowering the threshold for TCR responses, TCPTP deficiency might render CD8$^+$ T cells with low affinity for self-pMHC as "high-affinity" T cells with an increased propensity for overt autoreactivity and disease. Thus, enhanced T cell homeostasis/LIP may also account for the development of autoimmune disease in *Lck*-Cre;*Ptpn2*$^{fl/fl}$ mice. This would be in keeping with the previously established potential of lymphopenia to contribute to the development of autoimmune diseases, such as type 1 diabetes, rheumatoid arthritis, Crohn's disease, and systemic lupus erythematosus (70).

It is important to note that the autoimmune phenotype in *Lck*-Cre;*Ptpn2*$^{fl/fl}$ mice was evident on a "non-autoimmune" C57BL/6 strain background. Autoimmunity occurred despite the increased number of regulatory T cells and was not associated with a defect in regulatory T cell function. A SNP in *PTPN22* (encodes LYP/PEP) contributes to the development of several autoimmune diseases, including type 1 diabetes, rheumatoid arthritis, and lupus (32). However, in contrast to *Lck*-Cre;*Ptpn2*$^{fl/fl}$ mice, PEP$^{-/-}$ mice do not develop inflammation and organ damage on a C57BL/6 background (29). Our studies indicate that TCPTP is an important negative regulator of TCR and SFK signaling in naive T cells. In contrast, PEP is redundant in naive T cells and functions to dephosphorylate and inactivate Lck in effector/memory T cells (29). TCPTP's regulation of TCR/SFK signaling in naive T cells may be key to the onset of autoimmunity in *Lck*-Cre;*Ptpn2*$^{fl/fl}$ mice. However, TCPTP has also been implicated in the regulation of JAK/STAT (64) and TNF signaling (48), and we cannot exclude the possibility that enhanced cytokine signaling may also contribute to disease progression. Indeed, IL-2–induced STAT5 signaling and responses were increased in TCPTP-deficient CD4$^+$ and CD8$^+$ T cells. Although STAT5 can serve as a TCPTP substrate (63), the enhanced IL-2–induced responses were most likely due to elevated TCR-induced expression of the IL-2 receptor. STAT6 can also serve as a TCPTP substrate (71), but we found no overt difference in IL-4–induced STAT6 signaling and responses in CD4$^+$ T cells in vitro. Additional studies are needed to specifically determine the contributions of potentially altered cytokine signaling in *Lck*-Cre;*Ptpn2*$^{fl/fl}$ mice. Interestingly, TCPTP differentially contributed to naive CD4$^+$ versus CD8$^+$ T cell responses. TCR-induced activation and proliferation were enhanced in both CD4$^+$ and CD8$^+$ *Lck*-Cre;*Ptpn2*$^{fl/fl}$ T cells, but TCR threshold responses were only evident in CD8$^+$ T cells. This may been due to TCPTP differentially contributing to the regulation of Lck and Fyn, or possibly other substrates in CD4$^+$ versus CD8$^+$ T cells. Furthermore, our studies do not exclude the possibility that additional PTPs contribute to the regulation of SFKs in naive T cells. Indeed, we suggest that TCPTP regulates responses to low-affinity antigens and that other PTPs may have a more prominent role in regulating TCR signaling/responses to high-affinity or foreign antigens (since CD8$^+$ proliferation induced by saturating concentrations of crosslinking antibody, co-stimulation, or high-affinity peptide antigen were modestly affected by TCPTP deficiency). One possible candidate is SHP-1, which dephosphorylates Lck, ZAP-70, and LAT (24, 26, 27) and has recently been show to regulate the magnitude of a primary CD8$^+$ T cell response (72).

The TCR proximal SFKs Lck and Fyn are essential for T cell immunity and naive T cell homeostasis (2, 3, 8, 9, 73). Conversely, sustained Lck activation can result in a loss of tolerance and the onset of disease (3, 74). We propose that elevated TCR-induced SFK activation in TCPTP-deficient T cells may be responsible for the inflammatory and autoimmune phenotype in *Lck*-Cre;*Ptpn2*$^{fl/fl}$ mice. In humans, genome-wide association studies have linked *PTPN2* SNPs to autoimmune disorders (33–35), whereas the type 1 diabetes–associated *PTPN2* variant rs1893217(C) has been linked to a decrease in *PTPN2* message in CD4$^+$CD45RO$^+$ T cells (36). Although STAT5 can serve as a substrate for TCPTP (63), surprisingly the decreased *PTPN2* expression in the type 1 diabetes variant has been associated with decreased IL-2–induced STAT5 signaling (36). Although the molecular basis for this apparent defect in STAT5 signaling remains unclear (36), a possible consequence may be perturbations in the development/homeostasis of regulatory T cells that prevent autoimmunity (17). In this study, we delineate an alternate mechanism whereby TCPTP deficiency may contribute to the breakdown of immunological tolerance. Our studies highlight TCPTP's role in T cell development and function and establish its capacity to set the threshold for TCR-induced responses for the prevention of autoimmune and inflammatory diseases.

Methods

Materials. PMA, ionomycin, propidium iodide, and mouse α-tubulin (Ab-5) were purchased from Sigma-Aldrich. Mouse α–phospho-ERK1/2 and rabbit α–phospho-SFK (Y418), α–ZAP-70, and α-Fyn were from Cell Signaling Technology; rabbit α–phospho-Lck (Y394) (sc-101728) and mouse α-Lck (sc-433), α-ERK2 (sc-1647), α-CD3ε (sc-20047), and α-actin (sc-1616) were from Santa Cruz Biotechnology Inc.; mouse α–human CD3ε (OKT3) was from eBioscience; hamster α–mouse CD3ε (145-2C11) and hamster α–mouse CD28 were from BD Biosciences; and mouse α-TCPTP (6F3) was from Medimabs. The mouse ANA (anti-nuclear antibodies) Ig's (total IgA+G+M) ELISA Kit was purchased from Alpha Diagnostic International and the Transaminase CII kit from Wako Pure Chemical. The wild-type and mutant Lck and Fyn plasmids were provided by T. Mustelin (Amgen Inc., Seattle, Washington, USA), α-CD3ε and α-CD28 by A. Strasser (Walter and Eliza Hall Institute, Melbourne, Victoria, Australia), and α-TCPTP (CF4) by N.K. Tonks (Cold Spring Harbor Laboratory, Cold Spring Harbor, New York, USA).

Mice. We maintained mice on a 12-hour light/12-hour dark cycle in a temperature-controlled high barrier facility with free access to food and water. We used aged-matched and, where indicated, sex-matched mice for all experiments. *Ptpn2*$^{-/-}$ mice on a 129/Sv × BALB/c mixed background (38) were backcrossed onto a BALB/c background for 8 generations. *Ptpn2*$^{-/-}$ mice were genotyped as described previously (38). The *Lck*-Cre (originating from James D. Marth's laboratory, UCSD, La Jolla, California, USA; refs. 40, 41) and TCR (OT-I and OT-II) transgenic mice on C57BL/6J backgrounds were gifts from W. Alexander and W. Heath (Walter and Eliza Hall Institute).

Ptpn2$^{fl/+}$ *mice*. We used a 129/SvJ mouse BAC genomic library clone (pBeloBAC11, Incyte Genomics) for the generation of a targeting construct (75) that incorporated *loxP* sites flanking exons (ex) 5 and 6 and a neomycin resistance cassette flanked by FRT sites (Figure 1). The linearized targeting construct was electroporated into Bruce-4 (C57BL/6J) ES cells, and correctly targeted clones were injected into BALB/c blastocysts. High-percentage male chimeras were mated with C57BL/6J mice to produce *Ptpn2*$^{fl/+}$ offspring and subsequently with FLPe mice (C57BL/6) to excise the neomycin resistance cassette (75).

Ptpn2$^{fl/+}$ mice were mated with *Lck*-Cre mice for the conditional ablation of TCPTP in T cells. PCR was used to monitor for the floxed allele and the Cre transgene (75). Tissues of experimental mice were analyzed by immunoblotting for TCPTP expression. TCPTP was effectively deleted in thymocytes and T cells in more than 90% of cases, and only mice with less than 90% TCPTP deletion were used for the indicated analyses; TCPTP deletion was not evident in other tissues, including B cells, macrophages, monocytes, granulocytes, dendritic cells, spleen, kidney, pancreas, muscle, liver, heart, brain, lung, adipose tissue, salivary gland, and tail (Figure 1, Supplemental Figures 1 and 15).

Flow cytometry. Single-cell suspensions from freshly dissected thymi, spleens, and LNs were obtained by gently compressing samples between frosted glass slides and washing with cold PBS supplemented with 0.2% (w/v) BSA or 2% (v/v) FBS (CSL); thymocytes were homogenized further with an 18G needle. The resulting cell suspensions were recovered by centrifugation (330 *g*, 5 minutes at 4°C) and cell counts determined using a Z2 Coulter Counter (Beckman Coulter). Hepatic lymphocytes were isolated from perfused livers cut it into small pieces and strained through a 200-μm sieve. Hepatocytes and cell debris were removed using a 33% Percoll (GE Healthcare) gradient at room temperature. Red blood cells were removed using red blood cell lysing buffer (Sigma-Aldrich).

For surface staining, cells were resuspended in PBS/2% FBS containing the antibody cocktail (Supplemental Methods), incubated on ice for 20 minutes, washed in PBS/2% FBS, and analyzed by flow cytometry. Data were collected on LSR II (BD Biosciences) or Cytomics FC500 (Beckman Coulter) flow cytometers and analyzed using CellQuest Pro, FACSDiVa (BD Biosciences), or FlowJo7 (Tree Star Inc.) software. For cell sorting, an Influx or FACSDiVa Vantage (BD Biosciences) sorter was used.

T cell isolation. Naive (CD44^{lo}) CD8$^+$ T cells used for TCR signaling and proliferation assays were purified from pooled LNs by FACS with an Influx Sorter (BD Biosciences). DP and CD8$^+$SP thymocytes were also purified by FACS. Naive CD8$^+$ T cells and DP thymocytes were routinely tested for purity (>99%). The purity for FACS-purified CD8$^+$SP thymocytes was greater than 95%.

For assessment of TCR signaling in CD8$^+$SP thymocytes, cells were purified using an autoMACS (Miltenyi Biotec). In brief, thymocytes were incubated with α-CD4–PE, followed by the addition of α-PE–conjugated MicroBeads. CD4$^+$SP and DP thymocytes were depleted, and the fraction containing DN and CD8$^+$SP thymocytes was labeled with α-CD8–PE, followed by incubation with α-PE–conjugated MicroBeads. CD8$^+$SP thymocytes were obtained using the autoMACS positive selection program. The purity of CD8$^+$SP cells was 88%–93%; contamination with CD4$^+$SP and DP thymocytes was less than 1% and that of DN thymocytes was 6%–12%.

TCR signaling and proliferation. For signaling assays, single-cell suspensions (1×10^7 to 2×10^7) were crosslinked with 0.5–2.5 μg/ml α–hamster CD3ε for 0–90 minutes at 37°C. After stimulation, cells were washed with ice-cold PBS and lysed in modified RIPA buffer (50 mM HEPES pH 7.4, 1% [v/v] Triton X-100, 1% [v/v] sodium deoxycholate, 0.1% [v/v] SDS, 150 mM NaCl, 10% [v/v] glycerol, 1.5 mM $MgCl_2$, 1 mM EGTA, 50 mM NaF, 1 mM sodium vanadate) plus protease inhibitors (leupeptin [5 μg/ml], pepstatin A [1 μg/ml], aprotinin [1 μg/ml], 1 mM benzamadine, 2 mM phenylmethysulfonyl fluoride) and processed for immunoblot analysis using the specified antibodies.

For an assessment of cellular proliferation by [^{3}H]thymidine incorporation, thymocytes (2×10^5 to 4×10^5) were resuspended in 0.2 ml complete RPMI 1640 medium (RPMI 1640 [Sigma-Aldrich] supplemented with 10% [v/v] heat-inactivated FBS [CSL], 1× non-essential amino acids [Sigma-Aldrich], 1 mM sodium pyruvate, 2 mM L-glutamine [Invitrogen], 50 μM β-mercaptoethanol plus 100 U/ml penicillin and 100 μg/ml streptomycin]) and plated onto round-bottom 96-well plates (BD Biosciences) coated with α-CD3ε (0–10 μg/ml) and α-CD28 (0–10 μg/ml) and incubated at 37°C, 5% CO_2 for 48 hours. Cells were then pulsed with 1 μCi [^{3}H]thymidine (Amersham Biosciences) for 16 hours and harvested using a Tomtec Mach IIM Cell Harvester and analyzed on a scintillation counter.

For an assessment of cellular proliferation by CFSE (Molecular Probes, Invitrogen) dilution, lymphocytes (1×10^7 to 5×10^7/ml) were resuspended in PBS supplemented with 2% (v/v) FBS and 2–5 μM CFSE for 5 minutes at room temperature. Cells were then washed twice with PBS supplemented with 5% (v/v) FBS and stimulated with plate-bound α-CD3ε (0–10 μg/ml) with or without α-CD28 (0–2.5 μg/ml) in complete RPMI medium for 72 hours and processed for flow cytometric analysis.

Naive OT-I and OT-II T cell proliferation and adoptive transfer. The in vitro proliferative responses of naive (CD44^{lo}) CD8$^+$ OTI LN T cells to SIINFEKL (N4) or the altered peptide ligands SIYNFEKL (Y3) and SIIQFEKL (Q4) (JPT Peptide Technologies) were assessed by CFSE dilution. CFSE-labeled cells (5×10^4) were incubated with the indicated concentrations of peptides for 48 hours for an assessment of cell division by flow cytometry.

For assessment of the in vivo proliferative responses of naive (CD44^{lo}) CD8$^+$ OT-I and (CD44^{lo}) CD4$^+$ OT-II LN T cells to the N4 or Y3 peptide ligands and OVA protein, respectively, CFSE-labeled cells (2×10^6) from 3- to 4-week-old female mice were transferred intravenously into 6-week-old syngeneic female recipients. After 24 hours, the recipient mice were immunized with 1.25–2.5 μg N4 versus Y3 or 25–50 μg OVA, and CFSE dilution was assessed in isolated cell suspension at 48–72 hours after immunization by flow cytometry. Proliferating donor CD8$^+$ OT-I and CD4$^+$ OT-II T cells were identified by gating for CD8$^+$ or CD4$^+$ TCRvα2$^+$ CFSE$^+$ cells.

Plasmids. pMT2, TCPTP-pMT2, and TCPTP-D182A-pMT2 constructs have been described previously (50). Lck-pJ3Ω and Lck-Y505F-pJ3Ω were generated by PCR using Platinum *Pfx* DNA Polymerase (Invitrogen) and Lck-pEF/HA and Lck-Y505F-pEF/HA as templates, respectively. For cloning the human wild-type and mutant Lck cDNAs into pJ3Ω, the oligonucleotides incorporated a *Hind*III site immediately 5′ to the initiating codon (5′-CGCCGCAAGCTTATGGGCTGTGGCTG-CAGCTCA-3′) and a *Kpn*I site immediately 3′ to the terminating codon (5′-CGCCGCGGTACCTCAAGGCTGAGGCTGGTACTGG-3′). The *Hind*III/*Kpn*I-digested PCR products were cloned into the *Hind*III/*Kpn*I sites of pJ3Ω.

Immunoprecipitations. Thymocytes (2×10^7 to 5×10^7) were lysed in standard immunoprecipitation lysis buffer (20 mM Tris pH 7.5, 1% Triton X-100, 0.5% [w/v] NP40, 150 mM NaCl, 50 mM NaF) plus protease inhibitors, with or without 1 mM sodium vanadate, and clarified by centrifugation (16,000 *g* for 15 minutes at 4°C), and Lck (mouse α-Lck, sc-433, Santa Cruz Biotechnology Inc.) was immunoprecipitated as described previously (50) and processed for immunoblot analysis.

Substrate trapping. COS1 cells and Jurkat E6.1 T cells were cultured at 37°C and 5% CO_2 in Dulbecco's modified Eagle's and RPMI-1640 medium, respectively, containing 5% (v/v) FBS, 100 U/ml penicillin, and 100 μg/ml streptomycin. Cells were transfected as indicated by electroporation (transfection efficiencies of approximately 75%–90% for COS1 and approximately 70% for Jurkat T cells) as described previously (50). After 48 hours, cells were lysed in substrate-trapping lysis buffer and precleared with Pansorbin (Calbiochem), and cell lysates or TCPTP immunoprecipitates (CF4) were processed as described previously (50).

Cytokine detection. Serum cytokines from 48-week-old mice were detected with the BD Cytometric Bead Array kit according to the manufacturer's instructions (BD Biosciences).

Histology. Lung and liver tissue from 40- and 48-week-old mice were fixed with formalin and embedded in paraffin. Tissue sections were stained with hematoxylin, followed by eosin counterstaining. Sections were analyzed using a BX51 Olympus slide system and OlyVIA imaging software (Olympus).

Statistics. Statistical analyses were performed using GraphPad Prism software and the nonparametric, unpaired, 2-tailed Mann-Whitney *U* test, where $n \geq 4$, and an unpaired, 2-tailed Student's *t* test, where $n = 3$. *P* values less than 0.05 were considered significant.

Study approval. All experiments were performed in accordance with the National Health and Medical Research Council (NHMRC) Australian Code of Practice for the Care and Use of Animals. All protocols were approved by the Monash University School of Biomedical Sciences Animal Ethics Committee.

Acknowledgments

We thank A. Strasser, W. Langdon, F. Carbone, W. Heath, and S. Turner for helpful discussions. This work was supported by the NHMRC of Australia (to T. Tiganis, D.I. Godfrey, and S.M. Russell); S.M. Russell is an Australian Research Council Future Fellow, and T. Tiganis and D.I. Godfrey are NHMRC Principal Research Fellows.

Received for publication June 14, 2011, and accepted in revised form October 7, 2011.

Address correspondence to: Tony Tiganis, Department of Biochemistry and Molecular Biology, School of Biomedical Sciences, Level 1, Building 77, Monash University, Victoria 3800, Australia. Phone: 61.3.9902.9332; Fax: 61.3.9902.9500; E-mail: Tony.Tiganis@med.monash.edu.au.

Sandra Galic's present address is: St Vincent's Institute, Fitzroy, Victoria, Australia.

Catherine van Vliet's present address is: Department of Microbiology and Immunology, University of Melbourne, Melbourne, Victoria, Australia.

1. Smith-Garvin JE, Koretzky GA, Jordan MS. T cell activation. *Annu Rev Immunol*. 2009;27:591–619.
2. Palacios EH, Weiss A. Function of the Src-family kinases, Lck and Fyn, in T-cell development and activation. *Oncogene*. 2004;23(48):7990–8000.
3. Salmond RJ, Filby A, Qureshi I, Caserta S, Zamoyska R. T-cell receptor proximal signaling via the Src-family kinases, Lck and Fyn, influences T-cell activation, differentiation, and tolerance. *Immunol Rev*. 2009;228(1):9–22.
4. Palmer E, Naeher D. Affinity threshold for thymic selection through a T-cell receptor-co-receptor zipper. *Nat Rev Immunol*. 2009;9(3):207–213.
5. Kerry SE, et al. Interplay between TCR affinity and necessity of coreceptor ligation: high-affinity peptide-MHC/TCR interaction overcomes lack of CD8 engagement. *J Immunol*. 2003;171(9):4493–4503.
6. Molina TJ, et al. Profound block in thymocyte development in mice lacking p56lck. *Nature*. 1992;357(6374):161–164.
7. Tewari K, Walent J, Svaren J, Zamoyska R, Suresh M. Differential requirement for Lck during primary and memory CD8+ T cell responses. *Proc Natl Acad Sci U S A*. 2006;103(44):16388–16393.
8. Lovatt M, Filby A, Parravicini V, Werlen G, Palmer E, Zamoyska R. Lck regulates the threshold of activation in primary T cells, while both Lck and Fyn contribute to the magnitude of the extracellular signal-related kinase response. *Mol Cell Biol*. 2006;26(22):8655–8665.
9. Seddon B, Legname G, Tomlinson P, Zamoyska R. Long-term survival but impaired homeostatic proliferation of Naive T cells in the absence of p56lck. *Science*. 2000;290(5489):127–131.
10. Hogquist KA, Baldwin TA, Jameson SC. Central tolerance: learning self-control in the thymus. *Nat Rev Immunol*. 2005;5(10):772–782.
11. Daniels MA, et al. Thymic selection threshold defined by compartmentalization of Ras/MAPK signalling. *Nature*. 2006;444(7120):724–729.
12. Jenkins MR, Tsun A, Stinchcombe JC, Griffiths GM. The strength of T cell receptor signal controls the polarization of cytotoxic machinery to the immunological synapse. *Immunity*. 2009;31(4):621–631.
13. Gett AV, Sallusto F, Lanzavecchia A, Geginat J. T cell fitness determined by signal strength. *Nat Immunol*. 2003;4(4):355–360.
14. Zehn D, Lee SY, Bevan MJ. Complete but curtailed T-cell response to very low-affinity antigen. *Nature*. 2009;458(7235):211–214.
15. Rosette C, et al. The impact of duration versus extent of TCR occupancy on T cell activation: a revision of the kinetic proofreading model. *Immunity*. 2001;15(1):59–70.
16. Aleksic M, et al. Dependence of T cell antigen recognition on T cell receptor-peptide MHC confinement time. *Immunity*. 2010;32(2):163–174.
17. Malek TR. The biology of interleukin-2. *Annu Rev Immunol*. 2008;26:453–479.
18. Pingel JT, Thomas ML. Evidence that the leukocyte-common antigen is required for antigen-induced T lymphocyte proliferation. *Cell*. 1989; 58(6):1055–1065.
19. Koretzky GA, Picus J, Thomas ML, Weiss A. Tyrosine phosphatase CD45 is essential for coupling T-cell antigen receptor to the phosphatidyl inositol pathway. *Nature*. 1990;346(6279):66–68.
20. Mustelin T, Coggeshall KM, Altman A. Rapid activation of the T-cell tyrosine protein kinase pp56lck by the CD45 phosphotyrosine phosphatase. *Proc Natl Acad Sci U S A*. 1989;86(16):6302–6306.
21. McNeill L, et al. The differential regulation of Lck kinase phosphorylation sites by CD45 is critical for T cell receptor signaling responses. *Immunity*. 2007;27(3):425–437.
22. D'Oro U, Ashwell JD. Cutting edge: the CD45 tyrosine phosphatase is an inhibitor of Lck activity in thymocytes. *J Immunol*. 1999;162(4):1879–1883.
23. Zikherman J, et al. CD45-Csk phosphatase-kinase titration uncouples basal and inducible T cell receptor signaling during thymic development. *Immunity*. 2010;32(3):342–354.
24. Stefanova I, Hemmer B, Vergelli M, Martin R, Biddison WE, Germain RN. TCR ligand discrimination is enforced by competing ERK positive and SHP-1 negative feedback pathways. *Nat Immunol*. 2003;4(3):248–254.
25. Chiang GG, Sefton BM. Specific dephosphorylation of the Lck tyrosine protein kinase at Tyr-394 by the SHP-1 protein-tyrosine phosphatase. *J Biol Chem*. 2001;276(25):23173–23178.
26. Plas DR, et al. Direct regulation of ZAP-70 by SHP-1 in T cell antigen receptor signaling. *Science*. 1996;272(5265):1173–1176.
27. Kosugi A, Sakakura J, Yasuda K, Ogata M, Hamaoka T. Involvement of SHP-1 tyrosine phosphatase in TCR-mediated signaling pathways in lipid rafts. *Immunity*. 2001;14(6):669–680.
28. Gjorloff-Wingren A, Saxena M, Williams S, Hammi D, Mustelin T. Characterization of TCR-induced receptor-proximal signaling events negatively regulated by the protein tyrosine phosphatase PEP. *Eur J Immunol*. 1999;29(12):3845–3854.
29. Hasegawa K, Martin F, Huang G, Tumas D, Diehl L, Chan AC. PEST domain-enriched tyrosine phosphatase (PEP) regulation of effector/memory T cells. *Science*. 2004;303(5658):685–689.
30. Kung C, et al. Mutations in the tyrosine phosphatase CD45 gene in a child with severe combined immunodeficiency disease. *Nat Med*. 2000;6(3):343–345.
31. Tchilian EZ, Wallace DL, Wells RS, Flower DR, Morgan G, Beverley PC. A deletion in the gene encoding the CD45 antigen in a patient with SCID. *J Immunol*. 2001;166(2):1308–1313.
32. Bottini N, Vang T, Cucca F, Mustelin T. Role of PTPN22 in type 1 diabetes and other autoimmune diseases. *Semin Immunol*. 2006;18(4):207–213.
33. Todd JA, et al. Robust associations of four new chromosome regions from genome-wide analyses of type 1 diabetes. *Nat Genet*. 2007;39(7):857–864.
34. Smyth DJ, et al. Shared and distinct genetic variants in type 1 diabetes and celiac disease. *N Engl J Med*. 2008;359(26):2767–2777.
35. WTCCC. Genome-wide association study of 14,000 cases of seven common diseases and 3,000 shared controls. *Nature*. 2007;447(7145):661–678.
36. Long SA, et al. An autoimmune-associated variant in PTPN2 reveals an impairment of IL-2R signaling in CD4(+) T cells. *Genes Immun*. 2011;12(2):116–125.
37. Kleppe M, et al. Deletion of the protein tyrosine phosphatase gene PTPN2 in T-cell acute lymphoblastic leukemia. *Nat Genet*. 2010;42(6):530–535.
38. You-Ten KE, et al. Impaired bone marrow microenvironment and immune function in T cell protein tyrosine phosphatase-deficient mice. *J Exp Med*. 1997;186(5):683–693.
39. Heinonen KM, et al. T-cell protein tyrosine phosphatase deletion results in progressive systemic inflammatory disease. *Blood*. 2004; 103(9):3457–3464.
40. Hennet T, Hagen FK, Tabak LA, Marth JD. T-cell-specific deletion of a polypeptide N-acetylgalactosaminyl-transferase gene by site-directed recombination. *Proc Natl Acad Sci U S A*. 1995;92(26):12070–12074.
41. Gu H, Marth JD, Orban PC, Mossmann H, Rajewsky K. Deletion of a DNA polymerase beta gene segment in T cells using cell type-specific gene targeting. *Science*. 1994;265(5168):103–106.
42. Aliahmad P, Kaye J. Development of all CD4 T lineages requires nuclear factor TOX. *J Exp Med*. 2008;205(1):245–256.
43. Hogquist KA, Jameson SC, Heath WR, Howard JL, Bevan MJ, Carbone FR. T cell receptor antagonist peptides induce positive selection. *Cell*. 1994;76(1):17–27.
44. Barnden MJ, Allison J, Heath WR, Carbone FR. Defective TCR expression in transgenic mice constructed using cDNA-based alpha- and beta-chain genes under the control of heterologous regulatory elements. *Immunol Cell Biol*. 1998;76(1):34–40.
45. Woodland D, Happ MP, Bill J, Palmer E. Requirement for cotolerogenic gene products in the

clonal deletion of I-E reactive T cells. *Science*. 1990;247(4945):964–967.
46. Fink PJ, Swan K, Turk G, Moore MW, Carbone FR. Both intrathymic and peripheral selection modulate the differential expression of V beta 5 among CD4+ and CD8+ T cells. *J Exp Med*. 1992; 176(6):1733–1738.
47. Calnan BJ, Szychowski S, Chan FK, Cado D, Winoto A. A role for the orphan steroid receptor Nur77 in apoptosis accompanying antigen-induced negative selection. *Immunity*. 1995;3(3):273–282.
48. van Vliet C, et al. Selective regulation of tumor necrosis factor-induced Erk signaling by Src family kinases and the T cell protein tyrosine phosphatase. *Nat Immunol*. 2005;6(3):253–260.
49. Flint AJ, Tiganis T, Barford D, Tonks NK. Development of "substrate-trapping" mutants to identify physiological substrates of protein tyrosine phosphatases. *Proc Natl Acad Sci U S A*. 1997;94(5):1680–1685.
50. Tiganis T, Bennett AM, Ravichandran KS, Tonks NK. Epidermal growth factor receptor and the adaptor protein p52^{Shc} are specific substrates of T-cell protein tyrosine phosphatase. *Mol Cell Biol*. 1998;18(3):1622–1634.
51. Tiganis T, Bennett AM. Protein tyrosine phosphatase function: the substrate perspective. *Biochem J*. 2007;402(1):1–15.
52. Au-Yeung BB, et al. The structure, regulation, and function of ZAP-70. *Immunol Rev*. 2009;228(1):41–57.
53. Sugie K, Jeon MS, Grey HM. Activation of naive CD4 T cells by anti-CD3 reveals an important role for Fyn in Lck-mediated signaling. *Proc Natl Acad Sci U S A*. 2004;101(41):14859–14864.
54. Straus DB, Weiss A. Genetic evidence for the involvement of the lck tyrosine kinase in signal transduction through the T cell antigen receptor. *Cell*. 1992;70(4):585–593.
55. Lorenz U, Ravichandran KS, Burakoff SJ, Neel BG. Lack of SHPTP1 results in src-family kinase hyperactivation and thymocyte hyperresponsiveness. *Proc Natl Acad Sci U S A*. 1996;93(18):9624–9629.
56. Barnden MJ, Heath WR, Rodda S, Carbone FR. Peptide antagonists that promote positive selection are inefficient at T cell activation and thymocyte deletion. *Eur J Immunol*. 1994;24(10):2452–2456.
57. Ge Q, et al. Soluble peptide-MHC monomers cause activation of CD8+ T cells through transfer of the peptide to T cell MHC molecules. *Proc Natl Acad Sci U S A*. 2002;99(21):13729–13734.
58. Hommel M, Hodgkin PD. TCR affinity promotes CD8+ T cell expansion by regulating survival. *J Immunol*. 2007;179(4):2250–2260.
59. Oo YH, Adams DH. The role of chemokines in the recruitment of lymphocytes to the liver. *J Autoimmun*. 2010;34(1):45–54.
60. Sarkar S, Kalia V, Haining WN, Konieczny BT, Subramaniam S, Ahmed R. Functional and genomic profiling of effector CD8 T cell subsets with distinct memory fates. *J Exp Med*. 2008;205(3):625–640.
61. Carter JD, Neel BG, Lorenz U. The tyrosine phosphatase SHP-1 influences thymocyte selection by setting TCR signaling thresholds. *Int Immunol*. 1999;11(12):1999–2014.
62. Chong MM, et al. Suppressor of cytokine signaling-1 is a critical regulator of interleukin-7-dependent CD8+ T cell differentiation. *Immunity*. 2003;18(4):475–487.
63. Aoki N, Matsuda T. A nuclear protein tyrosine phosphatase TC-PTP is a potential negative regulator of the PRL-mediated signaling pathway: dephosphorylation and deactivation of signal transducer and activator of transcription 5a and 5b by TC-PTP in nucleus. *Mol Endocrinol*. 2002; 16(1):58–69.
64. Simoncic PD, Lee-Loy A, Barber DL, Tremblay ML, McGlade CJ. The T cell protein tyrosine phosphatase is a negative regulator of janus family kinases 1 and 3. *Curr Biol*. 2002;12(6):446–453.
65. Legname G, et al. Inducible expression of a p56Lck transgene reveals a central role for Lck in the differentiation of CD4 SP thymocytes. *Immunity*. 2000;12(5):537–546.
66. Hernandez-Hoyos G, Sohn SJ, Rothenberg EV, Alberola-Ila J. Lck activity controls CD4/CD8 T cell lineage commitment. *Immunity*. 2000;12(3):313–322.
67. Surh CD, Sprent J. Homeostasis of naive and memory T cells. *Immunity*. 2008;29(6):848–862.
68. Kassiotis G, Zamoyska R, Stockinger B. Involvement of avidity for major histocompatibility complex in homeostasis of naive and memory T cells. *J Exp Med*. 2003;197(8):1007–1016.
69. Kieper WC, Burghardt JT, Surh CD. A role for TCR affinity in regulating naive T cell homeostasis. *J Immunol*. 2004;172(1):40–44.
70. Datta S, Sarvetnick N. Lymphocyte proliferation in immune-mediated diseases. *Trends Immunol*. 2009;30(9):430–438.
71. Lu X, et al. T-cell protein tyrosine phosphatase, distinctively expressed in activated-B-cell-like diffuse large B-cell lymphomas, is the nuclear phosphatase of STAT6. *Mol Cell Biol*. 2007;27(6):2166–2179.
72. Fowler CC, Pao LI, Blattman JN, Greenberg PD. SHP-1 in T cells limits the production of CD8 effector cells without impacting the formation of long-lived central memory cells. *J Immunol*. 2010;185(6):3256–3267.
73. Seddon B, Zamoyska R. TCR signals mediated by Src family kinases are essential for the survival of naive T cells. *J Immunol*. 2002;169(6):2997–3005.
74. Filby A, et al. Fyn regulates the duration of TCR engagement needed for commitment to effector function. *J Immunol*. 2007;179(7):4635–4644.
75. Loh K, et al. Elevated hypothalamic TCPTP in obesity contributes to cellular leptin resistance. *Cell Metab*. 2011;14(5):684–699.